



Contents lists available at ScienceDirect

Marine and Petroleum Geology

journal homepage: www.elsevier.com/locate/marpetgeo

Tectonic and stratigraphic evolution of the Cretaceous Western South Atlantic

Pedro Kress^{a,*}, Octavian Catuneanu^b, Ricardo Gerster^{c,1}, Nestor Bolatti^a^a YPF SA Offshore Exploration, Macacha Güemes 515, C1106BKK, Buenos Aires, Argentina^b Department of Earth and Atmospheric Sciences, University of Alberta, 1-26 Earth Sciences Building, Edmonton, Alberta, T6G 2E3, Canada^c YPF SA, Argentina

ARTICLE INFO

Keywords:

Southwestern South Atlantic
Offshore Argentina
Cretaceous- paleogeography
Sequence stratigraphy
Volcanic divergent margin
Argentine Basin

ABSTRACT

The Cretaceous evolution of the Argentine margin between the Agulhas Malvinas Fracture Zone and the Rio de la Plata Fracture Zone is key in understanding the development of a volcanic divergent margin. In order to outline the evolution, more than 50000 km of 2D Seismic data were the foundation for the identification of the tectonic events and the sequence stratigraphic interpretation of the margin. However, ages of these events remain uncertain, as well data is limited to continental and shallow marine sequences with few biostratigraphic records.

Rifting during late Jurassic-early Cretaceous times preserved under the current shelf seems not to be mechanically linked to the crustal thinning, breakup and subsequent generation of oceanic crust, as rifts entered into sag stage before the onset of crustal breakup.

Four main turning points in the evolution of the passive margin have been identified: (i) crustal breakup associated with the SDRs emplaced during the late fault-extensional stage of the margin (ii) top of the first marine transgression creating accommodation for shallow marine carbonate and clastic deposits by Late Aptian times, followed by the development of a stratigraphic shelfbreak in overall shallow marine (300 m) paleowater depth during Albian times; (iii) a regional unconformity after which deep marine conditions with a structurally enhanced shelfbreak and thermohaline currents came into being (Late Cenomanian – Turonian), likely to be associated to final split off between SW Africa and the Malvinas plateau; (iv) a regional unconformity followed by a widespread transgression which marks the end of the Cretaceous (Maastrichtian-Danian) and a margin-wide reorganization of the sediment dispersal systems.

1. Introduction

The South Western South Atlantic corresponds to the present Argentine offshore, herein restricted to the southern section of the Austral segment in the sense of Moulin et al. (2010) between the Agulhas Malvinas fracture zone to the south and the Rio de la Plata fracture zone to the north (Fig. 1).

A clear outline of the tectonic and stratigraphic evolution during the Cretaceous of this segment is key in the understanding of the South Atlantic breakup and its early stages of development. Although in the past significant volume of data (both wells and seismic data) have been gathered from the African conjugate margin, on the Argentine margin, until recently only a coarse grid of seismic data existed in the deep offshore. A new data grid shot by Spectrum ASA together with existing

data has shed new light on the area, promoting new evolutionary models and hypothesis which contribute to a better understanding of the area.

The evolution of the Western South Atlantic margin during the Cretaceous yields constraints on the regional understanding of all the variables involved in the petroleum system expected for this margin.

The paper is aimed at proposing an evolutionary model for the depositional sequences present in the Argentine Basin and the eastern (outer) Colorado and Salado basins spanning Barremian Aptian to Danian times. This interval covers the early post-breakup history of the margin, well represented in the Argentine Basin and extending into the outer Colorado and Salado Basins (Fig. 1).

* Corresponding author.

E-mail address: pkress@ypf.com (P. Kress).¹ Offshore Exploration (retired).

<https://doi.org/10.1016/j.marpetgeo.2021.105197>

Received 21 February 2021; Received in revised form 18 June 2021; Accepted 19 June 2021

Available online 26 June 2021

0264-8172/© 2021 Elsevier Ltd. All rights reserved.

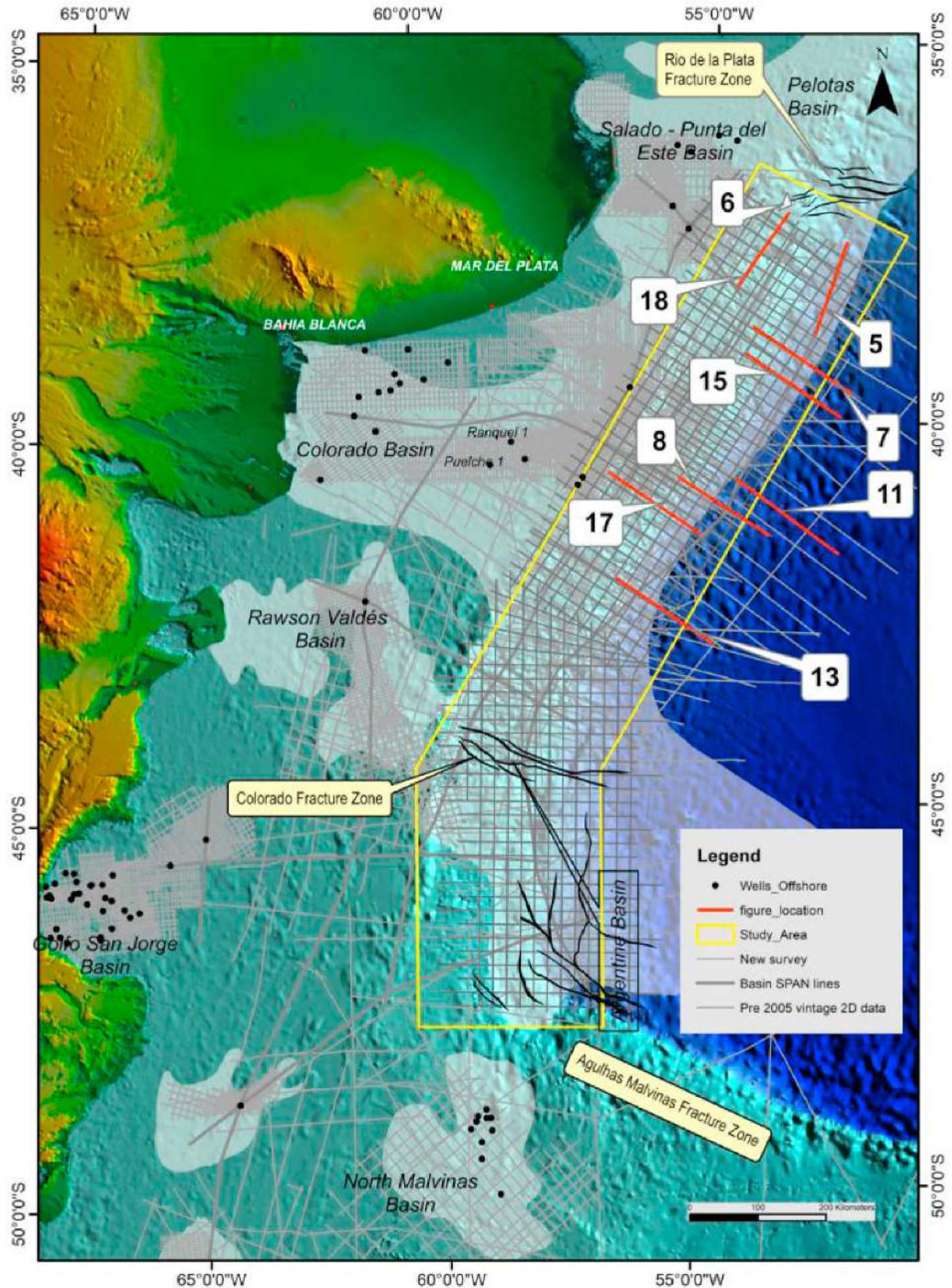


Fig. 1. Location of the study area and database used for this paper. Red lines correspond to the seismic sections and tracings; numbers relate to the figures in the text. Shaded areas represent basinal areas (rift and sag extent previous to breakup and the sedimentary wedge of the Argentine Basin). Wells shown on the map could only be used for correlation for the uppermost Cretaceous – lower Paleocene transgression. Wells labeled as Ranquel and Puelches refer to section 8.2. See text for further explanations. (For interpretation of the references to color in this figure legend, the reader is referred to the Web version of this article.)

2. Location and database

Fig. 1 shows a location map with the study area and the database used and from which the main conclusions and hypotheses of this paper were derived. In addition, published sources quoted in the text for the African conjugate margin were used to compare the pace of the opening of the South Atlantic.

The area covers 340000 km² and is located on the western margin of the South Atlantic. Under the broad Argentine shelf, the pre-breakup history is preserved through extensional basins, recording both the rift and sag stage. The current slope marks the western boundary of the deep water Argentine Basin, where the sedimentary wedge overlays the magmatic packages associated to the earliest stages of breakup and records the stratigraphic history along the margin.

More than 50,000 km of 2D seismic data from different vintages have been interpreted, with a focus on the outer shelf and adjacent slope and basin floor areas. Seismic data are of different vintages, where oldest surveys cover the shelf and only recently basin spanlines shot by ION Geophysical and a regional grid shot by Spectrum added critical information to the database. However, average spacing of the available data is in the order of 20 km, which is adequate for regional correlations but too coarse for a more detailed seismic facies interpretation.

Quality of the data is highly variable, depending on the age and purpose of each survey. Oldest records date back to 1970, along the slope in shallow water with relatively short streamers. Recording rarely exceeded 4 s and multiples were often not adequately corrected. Newer data imply a much more complete processing, geometry and streamer array, the details of which are beyond the purpose of this paper.

Wells drilled on the shelf could only be used for correlations within uppermost Cretaceous and Paleocene, as older post breakup sections drilled are continental deposits or highly reworked shallow-marine sequences without age diagnostic elements.

All seismic data have been interpreted in time as velocity models without well ties are not likely to yield an adequate depth conversion.

Correlation with events well defined in South Africa and Namibia are difficult to assess on the Argentine margin. Hinz et al. (1999) created the first markers and suggested ages based on regional assumptions. To date, for the Cretaceous exact age values still remain elusive. The same subdivision has been used by many authors along the margin (Morales et al., 2017 in Uruguay, Hernandez-Molina et al., 2009; Loeggering in the Colorado Basin; and recently Rodrigues et al., 2021, among many others).

Therefore, interpretation must rely on the analysis of seismic stacking patterns and only regional events can bracket the different evolutionary steps.

3. Regional and stratigraphic framework

North of the Agulhas Malvinas - Fracture Zone (AMFZ) the South-western South Atlantic margin represents a Volcanic Divergent Margin, extending northwards into the Pelotas Basin, outside of the study area (Fig. 1).

The AMFZ terminates against the Deseado craton splitting into a series of branches oriented towards the north that mark the southern boundary of the magmatic packages of the SDRs. SDRs are segmented by a series of fractures (Franke et al., 2007) whose paleogeographic implications are discussed in section 4.

Within these fractures, the Colorado Fracture Zone marks a change in the orientation of the SDRs (Fig. 3), which is interpreted as a feature predating the breakup and controlling the pace of northwards propagation of rifting and generation of oceanic crust.

The Rio de la Plata Fracture Zone is part of a significant sinistral offset of oceanic crust, probably a consequence of inherited structural grain from pre-breakup features.

During Barremian to Lower Paleocene times, the stratigraphic wedge developed on the outer crust, the SDRs and the oceanic crust,

experienced significant changes in accommodation and sediment supply, which record the evolution of this passive margin, as will be shown with more detail in section 4.

Fig. 2 is a chronostratigraphic chart, tied to Cretaceous regional events and based on the stacking patterns identified on seismic data. Nomenclature follows Catuneanu (2006), 2019a; 2019b). It summarizes qualitatively the evolution of the margin, considering that the evolution along and across the margin was strongly diachronous.

On the left side, ages (in million years) and color coding correspond to the International Chronostratigraphic Chart (Cohen et al., 2018). Ocean anoxic events (OAEs) identified in the South Atlantic together with the Paleocene Eocene thermal maximum (PETM, McInerney and Wing, 2011) have been put into the context of the South Atlantic evolution (Leckie et al., 2002). In addition, major tectonic processes such as clearing off the Malvinas plateau from Africa and further the subduction of the Aluk and Farallon plates along the western border of the South American plate have been added to highlight the regional context. For the Campanian-Danian interval, Ar/Ar dating of the Puelches volcanics (Lovecchio et al., 2018) has been incorporated as time constraint for the transgression, as well as U/U ages from tuffs deposited in the time equivalent transgressive interval in the Neuquén Basin (Aguirre-Urreta et al., 2011).

The sequence packages shown are interpreted as 2nd order cycles, with some higher frequency (i.e., 3rd order) events, although effective correlation can only be achieved by 2nd order regional events along the entire margin. These events for the Upper Cretaceous interval correspond to turning points in the evolution of the margin, herein regarded as the post-rift stage, which correlate with changes in accommodation and paleobathymetry.

Their stratigraphic meaning and the internal array of the bounded intervals will be discussed in the following sections, but briefly they correspond to:

- the breakup unconformity, which is a composite erosive surface at the top of the magmatic packages marking the end of the rift stage extending landward where it marks the onset of the passive margin stage. This unit might be equivalent to the composed surface of the AR1 marker (Hinz et al., 1999)
- the top of the first shallow-marine transgression during Barremian – Middle Aptian times. In many places this composed surface is equivalent to the AR2 marker (Hinz et al. op.cit.)
- a regional unconformity interpreted to be related to the clearing off the easternmost edge of the Malvinas platform from South Africa close to the Cenomanian-Turonian boundary, marking the onset of deep-water circulation and development of thermohaline currents and marine inflow across the Agulhas threshold. This feature seems to be roughly equivalent to what has been identified locally in the Colorado Basin (Sag I marker of Loeggering et al., 2013) but not extended along the whole margin.
- a Campanian-Maastrichtian unconformity followed by a regional transgression that covered most of southern South America, which has also been identified along the western South African margin. This feature is largely equivalent with the AR3 marker (Hinz et al., 1999; Franke et al., 2007).

4. Pre-breakup structural framework

To date, both along the Argentine margin and its conjugate African counterpart there is no evidence of major rifting underneath the emplacement of the seaward dipping reflectors (SDRs), which seemed to have occurred over overthinned albeit with minor previous fractured continental to transitional crust.

Fig. 3 shows a reconstruction of both margins close to M0 time (125 m.y., base of Aptian). Picks taken from Granot and Dymant (2015) were used to link both margins. For a better orientation, current topographic features were preserved.

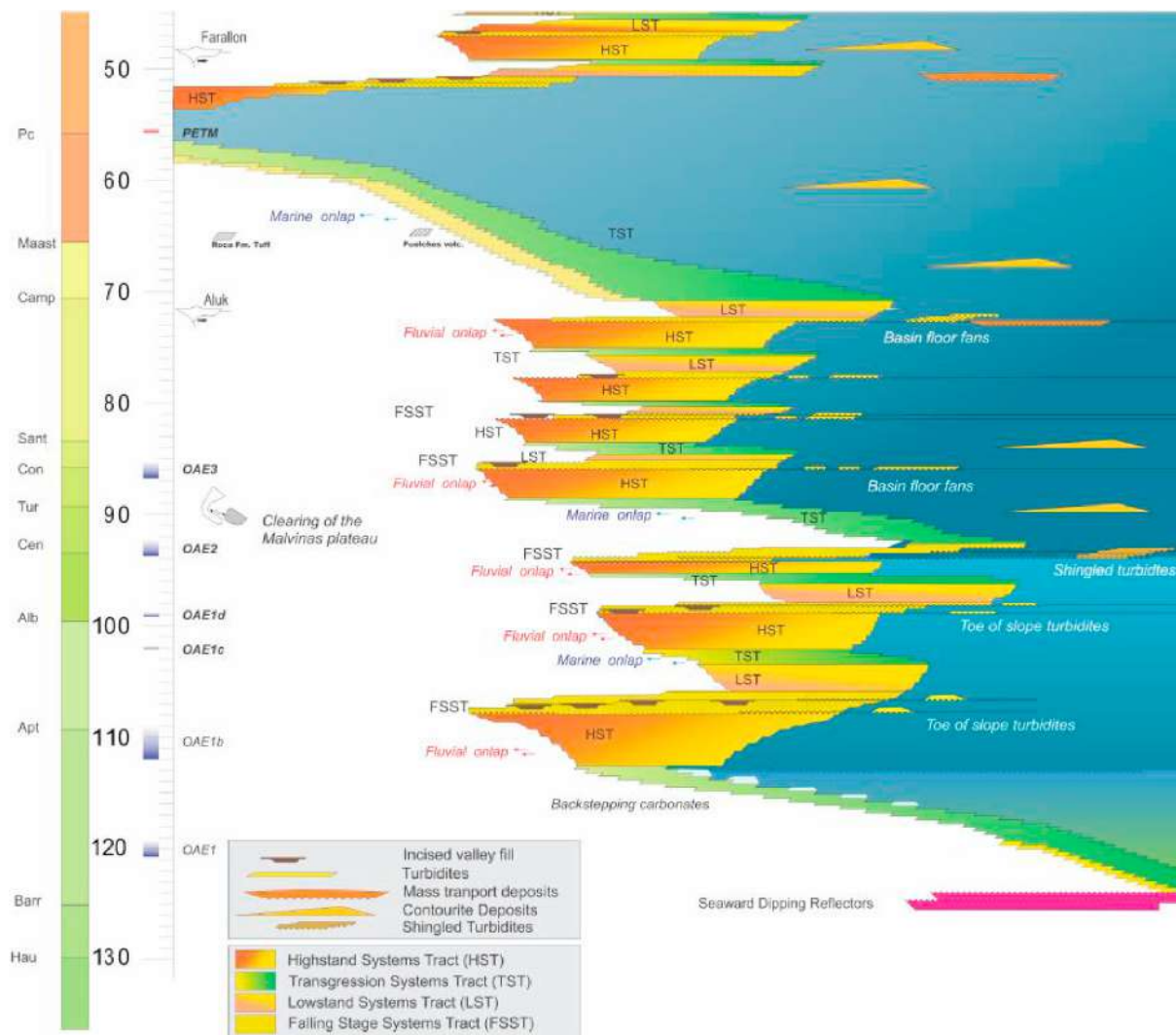


Fig. 2. Cretaceous to Paleogene chronostratigraphic chart of the western South Atlantic. Ages along the Y axis are expressed in million years. Clastic input elements are highlighted in brown to yellow colors, following a qualitative relationship of stacking patterns. Green colors correspond to the main transgressive intervals. Light blue segments represent backstepping carbonates during the Barremian Aptian transgression. On the left side, the geological timescale and the main Cretaceous Ocean anoxic events are highlighted. Due to the lack of well control, ages of the different events are tentative. See text for further explanations Modified from Kress et al. (2019)

The tectonic features shown correspond to the pre-breakup rift systems as well as the extent of the magmatic packages (SDRs) developed during the early stages of opening.

Data used for the African conjugate margin were taken from Broad et al. (2012), highlighting the extensional fault systems and related depocenters of the Oteniqua and Orange Basins. Distribution of the SDRs and bounding fractures (first-order segments) were taken from Koopmann et al. (2014a).

Data used for the Argentine margin integrate published and unpublished work. Outline of extensional faults and depocenters of the Salado Basin is based on Raggio et al. (2011) and data from the Colorado Basin are based on Gerster et al. (2011) and Lovecchio et al., (2020). The Rawson Valdes rift pattern is reinterpreted from Otis and Schneidermann (2000) and Continanzia et al. (2011), together with unpublished data.

Across the Argentine shelf, several rifts developed north of what later would become the Agulhas Malvinas fracture zone under the current shelf at high angles to the later continent-ocean transition (COT) zone, such as the Salado Colorado and Rawson-Valdés rifts. Age of onset is poorly constrained, but from regional reconstructions, extension in SW Gondwana started around the Jurassic-Cretaceous boundary, affecting a

highly heterogeneous crust composed of a mosaic of terranes accreted during Proterozoic to Upper Paleozoic times (Ramos, 2008; Lovecchio et al., 2020, for a detailed review). The rifts preserved under the present shelf entered into the sag stage before the emplacement of the SDRs, which are related to extensional faulting previous to the final crustal breakup. A later trend marked by smaller faults parallels the edge of the SDRs and might be related to local extensional processes linked to the SDR emplacement and rotation between South America and Africa during and after breakup (Fig. 3).

Along the South-western African margin, rifting processes have been identified in the Orange Basin landward and parallel to the SDRs, such as the A-J graben where wells drilled into Hauterivian fluvio-lacustrine sediments (Jungslager, 1999). The rifts are separated by a high from the SDRs further east.

Several of these rifts share biostratigraphic elements. Non-marine ostracods such as *Cypridea australis* have been identified in this rift system involving both margins as well as in the Hauterivian sections of the Neuquén and Golfo San Jorge basins (Mc Millan, 2003; Musacchio et al., 1990). A similar fauna though with higher degree of endemism has been reported from the North Malvinas Basin (Ayress and Whatley, 2014).

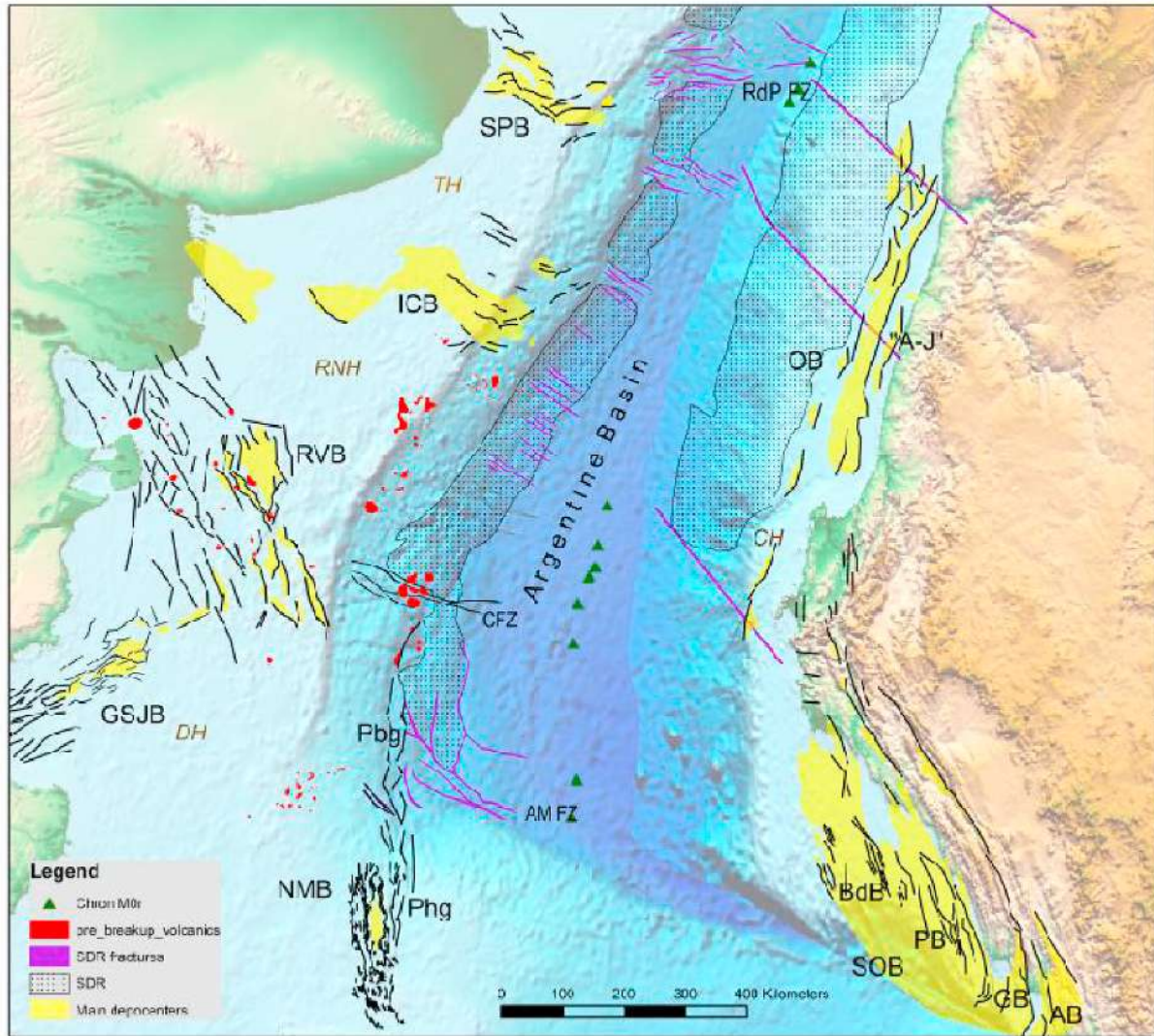


Fig. 3. Reconstruction of the early South Atlantic at M0 (Lower Aptian) times. The inset corresponds to the studied area. Present topography taken as a reference is sourced from <https://www.ngdc.noaa.gov/mgg/global/>. Green triangles are M0 magnetic anomaly picks taken from the latest update from Seton et al. (2014). Basin outlines are from different sources. See text for further references. Acronyms used correspond to the following basins/depocenters (clockwise listing): OB: Orange Basin; "A-J": A-J Graben landward of the main Orange Basin; SOB: Southern Outeniqua Basin; BdB: Bredasdorp Basin; PB: Pletmos Basin; GB: Gamtoos Basin; AB: Algoa Basin; AMFZ: Agulhas-Malvinas fracture zone; NMB: North Malvinas Basin; Phg: Phyllis Graben; Pbg: Piedrabuena Graben; GSJB: Golfo San Jorge Basin (Offshore); CFZ: Colorado Fracture Zone; RVB Rawson Valdés Basin; ICB Inner Colorado Basin; SPB Salado-Punta del Este Basin. (For interpretation of the references to color in this figure legend, the reader is referred to the Web version of this article.)

Northwards propagation of the breakup has been recognized for long (Müller and Nürnberg, 1991; Franke et al., 2007, and references therein), but the details still remain controversial. As mentioned above, in southwestern Gondwana Upper Jurassic regional extension resulted in a complex pattern of rifts, while breakup advanced stepwise along the present eastern African coast (Reeves et al., 2016). Propagation along the Agulhas fracture zone was buttressed by the Deseado High and redirected northwards.

South of the Salado Punta del Este Basin, there is no evidence of structural grain that might have controlled the direction of the breakup, which seems to have occurred stepwise, along linear segments, offset by fractures, where strain concentrated before renewed propagation along the next segment began (Koopmann et al., 2014). Northwards of the Punta del Este Basin, off the studied area along the Pelotas Basin and further north, the Proterozoic Dom Feliciano fold and thrust belt seems to have controlled the orientation of breakup, up to the Sao Paulo High. (Szatmari and Milani, 2016).

5. Onset of marine transgression in the western South Atlantic

The first marine transgression following the South Atlantic breakup is key in understanding the distribution of potential marine source rock as a critical element of the petroleum system expected for the deepwater Argentine Basin. As such, in the absence of calibration points such as wells or ties of the first sedimentary sequences towards the shelf, it is necessary to understand the stacking patterns to define the sedimentary processes during transgression and how the earliest shelf and shelf break developed.

5.1. The Southern Sea and the birth of the South Atlantic

Direct evidence and ages of the first transgression in the South Atlantic have been largely derived from the DSDP wells 360 and 361 in the Cape Basin (Bolli and Ryan, 1978) and the wells drilled in the northern Orange Basin (Mc Millan, 2003). To date, a few other commercial wells have been drilled across this section in the Orange Basin

(Hodgson and Intawong, 2013) proving its source rock potential.

It is uncertain, whether in the deepest areas, marine flooding was preceded by a lacustrine system, following a hypothesis of a subaerial stage of early spreading. In the Orange Basin, Brown et al. (1995) report the existence of evaporitic layers before the onset of the main drift phase.

It is also a matter of discussion whether flooding occurred across a subsiding area of the Malvinas platform or if it was actively driven by a fracture-controlled trench associated to the early activity of the Agulhas-Malvinas fracture zone.

Key in this evolution is the geologic history recorded in the Breddasdorp subbasin of the Outeniqua Basin (southern Africa), where marine transgression occurred around ~ 146 M.a. (Tithonian), while the basin was still in synrift stage (Mc Millan, 2003). The Outeniqua basin entered into sag stage by 126 M.a. (Lower Aptian), which corresponds to the 1At1 marker (breakup unconformity) in the south African literature (e.g., Brown et al., 1995; Broad et al., 2012).

Data and reconstructions from different sources highlight controversies. In the northern Orange Basin, Mc Millan et al. (1997) reports an Early Barremian – Early Aptian record on top of the SDRs in the Kudu area (124 M.a.), which further south seems not to be present. Absence of this section could be either due to early erosion or no deposition by restrictions on the marine flooding. According to McMillan et al. (1997) and Mc Millan (2003) transgression at the top of the SDRs is marked by an initially restricted anoxic relatively shallow (inner shelf) environment, which remained rather shallow, albeit with increasing open marine circulation until late Aptian times. The earliest restricted stages are characterized by a foraminiferal burst and high organic matter content, mixing marine and terrigenous sources. The same biostratigraphic evolutive pattern has been observed in the Malvinas Basin, which points to a connection between the Southern Sea and the embryonal South Atlantic (D. Ronchi, pers. Comm).

Heine et al. (2013), based on detailed kinematic models, propose first oceanic crust generation between the segment south of the Colorado Basin and the conjugate Orange Basin by 135 M.a. (~Valanginian).

Koopmann et al. (2014b) interpreted the magnetic anomalies in the Cape Basin and concluded that the earliest oceanic crust corresponds to the M10 anomaly (~134 M.a.). Alternatively, Moulin et al. (2010) interpreted in the same area the M7 anomaly (132 M.a.) as the age of the oldest oceanic crust. If the age indicated on top of the SDRs in the Kudu well and the interpretations of the magnetic anomalies are correct, the diachronous onset of oceanic crust generation along the Orange Basin lasted around ~10–12 M.y.

Along the South American continent-ocean crust transitional zone, magnetic anomalies show an overall lower susceptibility contrast, which makes their identification more difficult (Rabinowitz and La Brecque, 1979). Some magnetic trends have been associated to M7 and M4 anomalies (see Granot and Dymant, 2015 for an updated compilation). However, the origin of these anomalies might be challenged by new interpretations on the origin of the magnetized magmatic body (see section 6.1).

5.2. Seaward dipping reflectors and control on earliest marine transgressions

Previous seismic data clearly showed the volcanic nature of this divergent margin (Hinz et al., 1999; Franke et al., 2007 and references therein) by identifying on seismic lines dipping reflector packages interpreted as of magmatic origin and called seaward dipping reflectors or SDRs. They have been identified in other passive margins worldwide (Hinz, 1981; Menzies et al., 2002 for a review) and seem to be an end member of different mechanisms of continental breakup (Franke, 2012) and or crustal magmatic evolution (Tugend et al., 2018). Although the exact mechanism of the emplacement of the SDRs is still controversial, a working hypothesis relates them to significant pure shear crustal thinning with uprising mantle, until final rupture along discrete segments

that mark the pattern for the later continent-ocean transition. This rupture releases subaerially significant amounts of magmatic rock over relatively short time, probably synchronous to the development of the breakup unconformity. Depending on the amount of crustal thinning previous to fracturation, SDRs can evolve in several steps, developing wedges of different generations (Franke et al., 2007), before final ocean crust generation is achieved. With time, those packages tilt towards the fractures that originate them, according to the subsidence driven by the evacuation and collapse of the underlying magmatic chamber (Quirk et al., 2014). McDermott et al. (2018) show an alternative view for the origin of SDRs based on regional deep seismic reflection lines, suggesting two types of SDR emplacement, which might change from one into the other both in time and space.

In the South Atlantic, the fractures controlling the emplacement of the SDR wedges parallel the future landward edge of the oceanic crust. These segments are bounded along strike by fracture zones oriented at high angles, where the magmatic wedges dip parallel to the edge of the oceanic crust. The fracture zones seem to mark the stepwise propagation of the breakup, where sections of spreading alternate with rotational accommodation along the fracture zones (Franke et al., 2007), transforming them into *loci* of magmatic emplacement (Koopmann et al., 2014). Strike lines clearly show magmatic patterns which dip towards those fracture zones, which can be interpreted as magmatic centers with excess magmatism before further northward propagation. It is this superimposition of wedges with variable dip orientation that makes a discrimination of magmatic packages more complex.

Those fracture zones experienced changing strain according to the stress regimes that changed over time with the northwards formation of oceanic crust. Seismic data across fracture zones show transtensional and transpressive features that remained active long after the onset of oceanic crustal spreading. Cooling of magma underneath those fracture zones contributed to early subsidence and creation of restricted depocenters, during the earliest stages of marine transgression.

SDR emplacement seemed to have occurred during discrete time-steps (Franke et al., 2007). During the early stages of the SDR emplacement, magma rising below the young oceanic ridge in a mushroom shape created a buoyancy effect underneath the seaward dipping reflectors exposing them to subaerial and later submarine erosion.

A direct consequence of this model is that some of the fracture zones might have been places of deep, restricted marine environment, whereas the magmatic wedges along the edge of the oceanic crust remained exposed to erosion during the early stages.

Exposure of SDRs followed by submergence and transgression might have resulted in the deposition of backstepping coastal sandstones (e.g., analogous to the Springhill Formation in the Malvinas Basin (Galeazzi, 1998). For the Kudu area in the northern Orange Basin, where SDRs have been drilled, Wickens and Mac Lachlan (1990) report the existence of eolian and shallow-marine sandstones interlayered with magmatic packages.

Unlike a broad subsiding area envisioned by earlier regional reconstructions, the first areas to be flooded seemed to have been associated with the fracture zones that segment the SDR trends, during their stepwise northwards propagation.

Fig. 4 shows a paleogeographic reconstruction of the SW Atlantic Ocean, between the Agulhas-Malvinas fracture zone and the Rio de la Plata lineament, of the earliest marine transgression, around Barremian and Early Aptian times. The eastern boundary is given by the onlap on oceanic crust which, following most reconstructions, correlates broadly with the M0 anomaly of Lower Aptian (~125 M.a.) age.

The fracture zones and the segments they bound, follow the interpretation of Franke et al. (2007), although some of them have been modified from other sources and reinterpreted with new seismic data.

The southernmost segments which coincide with the Segment I from Franke et al. (2007) extend between the Agulhas-Malvinas fracture zone (AMFZ) and the Colorado Fracture zone (CFZ). The AMFZ fracture zone marks the northern boundary of the Malvinas plateau. Available seismic

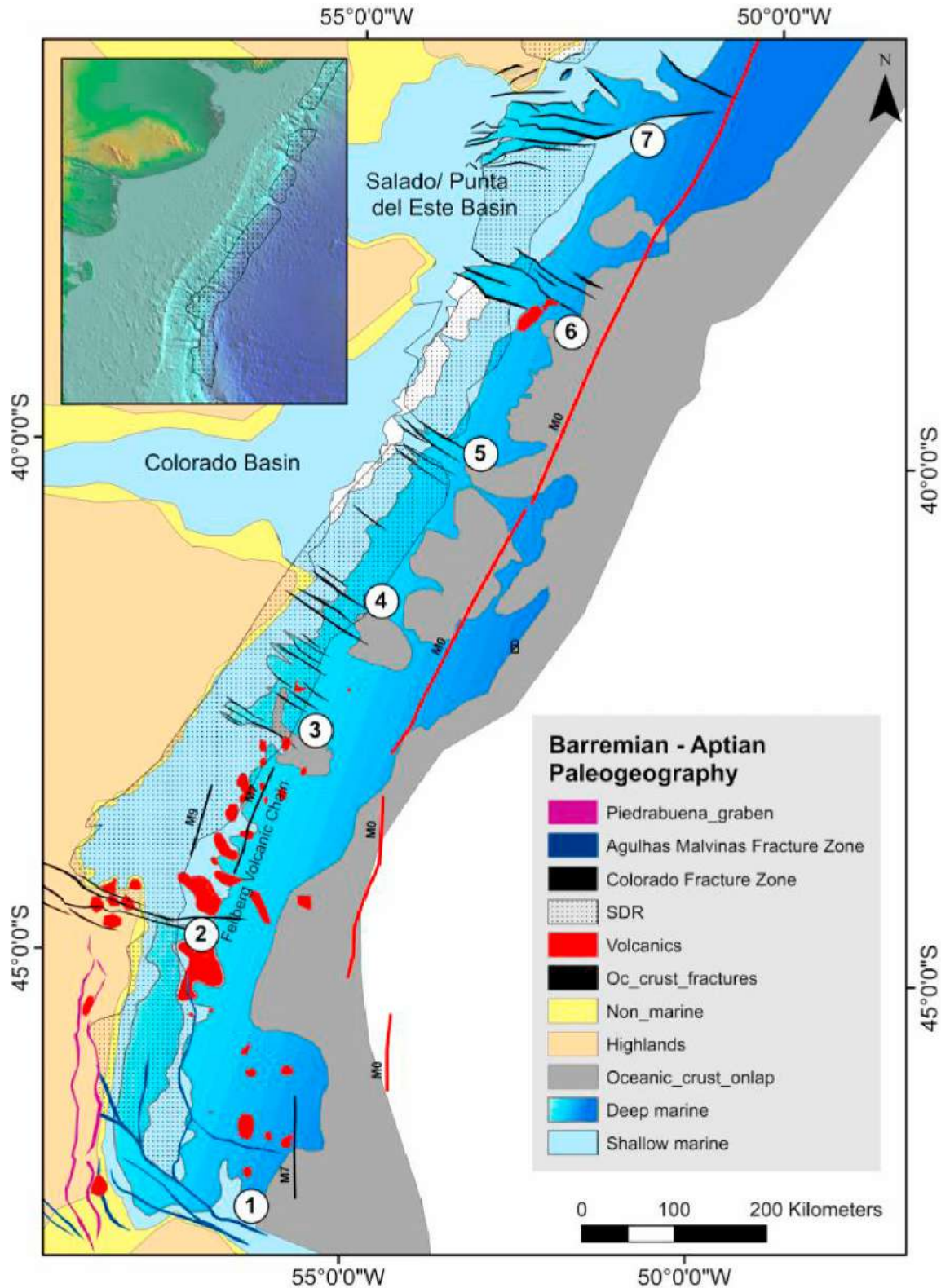


Fig. 4. Paleogeography of the earliest marine transgression in the SW Atlantic Ocean. The framework is determined by the main fracture zones, numbered from south to north. 1 Agulhas Malvinas fracture zone (AMFZ) 2 Colorado Fracture Zone (CFZ) 3 Bahía Blanca fracture zone (BFZ) 4 Ventana fracture zone (VFZ) 5 Tandil fracture zone (TFZ); 6 Salado fracture zone (SFZ) and 7 Rio de la Plata fracture zone (RPFZ). The fracture zones are related to the segmentation of the seaward dipping reflectors during their northwards propagation. The marine transgression is limited to the west by the onlap on top of the SDRs. Earliest transgression followed the graben structures associated with the fracture zones, which are well preserved north of the Colorado fracture zone. Shallow areas are fringing the first coastline. Between the Colorado Fracture Zone (CFT) and the Bahía Blanca fracture zone the eastern boundary of the SDRs is marked by the Feilberg Volcanic Chain, which is associated to crustal thinning, either during the transition from SDRs to normal oceanic crust as the youngest magmatic feeder systems or to a weakness zone, between landward thickened oldest and thinner oceanic crust to the east. The western boundary of the first marine transgression is given by its onlap on oceanic crust, likely to be related to the M0 anomaly of Upper Barremian – lower Aptian age. Magnetic anomalies taken from [Seton et al. \(2014\)](#).

data do not show any continuity into the crust of the Deseado Massif, but rather support a clear deflection towards the north.

Becker et al. (2012) already identified graben structures north of the North Malvinas Basin and related them to the early breakup of the South Atlantic. The North Malvinas Basin is a series of rifts that entered into sag stage previous to the breakup of the South Atlantic Lohr and Underhill (2015). The main graben, known as the Northern Rift Basin (NRB) is an elongated NS oriented graben which towards the north fades out into a series of smaller graben and horst structures, without connecting into the AMFZ shear zone. However, east of the NRB, which concentrates the main exploratory activity, and separated from it by the Eastern structural high, the Phyllis Graben (Jones et al., 2019), another elongated rift basin extends and deepens further north.

New seismic data show, that the southern tip of the AMFZ segment is marked by a complex network of strike slip faults, likely to be branches that separate from the AMFZ (Figs. 3 and 4). Those faults record a gradual change in orientation from E-W to NS outlining the future continent ocean transition (COT) zone. This change in orientation lead to thinning by transtension. Uplift along low angle NE dipping detachments expose the upper mantle, splitting off attenuated continental crust, from less thinned crust the west. The sheared crustal segments constitute a transform fault dominated segment, where SDRs are absent. Instead, controlled by a complex array of minor transtensional faults, a series of smaller volcanic bodies have been identified. The northernmost branch of the major strike slip faults marks the southern boundary of the SDRs.

These tectonic features compare with the conjugate margin, where Koopmann et al. (2014b) identified in the Cape Basin, north of the Agulhas Malvinas fracture zone, a segment without seaward dipping reflectors. They relate them to an initial breakup stage dominated by transform faults and state that the change from transform margin to a true volcanic divergent margin occurs over a few tens of kilometers.

Landwards of the transform margin and extending further north, a series of narrow, (30–40 km wide) N–S oriented graben structures developed. This so called “Piedrabuena graben” (Figs. 3 and 4), owns its name to the fact that it underlays the Piedrabuena terrace of the present seafloor (Hernández-Molina et al., 2009). It marks the western edge of the SDRs further north. It seems not to be related to the strike slip system of the AMFZ, as it extends south of the bend of the AMFZ, although some fault segments could have been reactivated by the termination of the strike slip fractures. Thus, it could either be an aborted branch of the Phyllis graben of the North Malvinas Basin or an independent rift, but in trend with the Phyllis graben.

The northern end of this rift structure is not clearly defined as it merges with chaotic reflectors, likely to be related to volcanic activity due south of the Colorado Fracture Zone. Also, there is no clear evidence that the rift remained active with tectonic driven subsidence during the emplacement of the SDRs.

Between the northernmost branch of the AMFZ shear zone and the Colorado Fracture Zone, SDR emplacement, expanded in width during its northward propagation. The Barremian transgression generated a shallow sea onlapping towards the west on the basement and the incipient SDRs further north; to the east it is bounded by a high, where the SDRs seemed to have been subaerially exposed prior to flooding. It is not clear whether this high can be interpreted as an outer high *sensu* Planke et al. (2000). East of this high, accommodation allowed deposition and preservation of a thicker Aptian record that onlaps on oceanic crust, which according to most reconstructions corresponds to the M0 anomaly of Lower Aptian age.

The Colorado Fracture Zone (Franke et al., 2007), which has no direct relationship with the Colorado Basin further north, marks (i) a change in the orientation of the SDR emplacement, from NS to NNE–SSW, and (ii) a significant offset counterclockwise of the edge of the SDRs, which is particularly apparent along the basement high at its southern edge. reduced to pole (RTP) magnetic anomaly maps show that this feature correlates with a change in magnetic pattern (Max et al.,

1999), which very likely corresponds to a deeply rooted crustal discontinuity, eventually representing the boundary between different terranes. Updip of the SDRs, extensional southwards dipping basement faults have been identified, which could be related to part of the Rawson rift system beneath the shelf further west (Fig. 4). Where these faults merge with the SDRs, they show pervasive volcanism.

Within the CFZ, reflector patterns interpreted as magmatic packages are faulted by several syndepositional fractures, and dip both towards the east as well as to the north and, less developed, to the south.

North of the CFZ a series of fractures segmenting different generations of SDRs extend up to the Rio de la Plata fracture zone, where a significant offset along a strike slip fault juxtaposes oceanic crust to the north against SDRs to the south. Franke et al. (2007) originally subdivided this part of the margin into three first-order segments by the Ventana, and Salado Basin. New seismic data confirm these features but also reveal more fracture zones, showing that strain accommodation during breakup occurred in a more diffuse distribution (Fig. 4).

Marine transgression followed first the lower, restricted areas associated with the fracture zones. They are interpreted as sites of crustal thinning and sourcing of magmatic packages during active extension, followed by subsidence during to concomitant cooling. They constitute areas with local restricted deep circulation where marine organic matter could have been preserved. According to Mc Millan (2003) in the area drilled by the Kudu wells in the Orange Basin, the oldest source rock intervals, P1 and P2 have a Barremian– Early Aptian age, elsewhere absent in the basin. It is probable that this source rock interval is somehow constrained to areas with higher subsidence rates such as the fracture zones.

The neighboring shallow areas on top of the SDRs were subsequently flooded as overall thermal cooling of the transitional crust proceeded.

The western (landward) boundary of the first marine transgression is given by the onlap on the SDRs and even continental crust inboard, subjected to subsidence during breakup. On top of the SDRs, flooding postdates subaerial exposure and was accompanied by wave-ravinement erosion. Where continental crust was flooded with concomitant sediment supply from fluvial systems, shallow marine transgressive sands were deposited. Where riverborne sediment supply was low, carbonate factories developed.

Between the CFZ and the Bahía Blanca Fracture Zone BFZ (Fig. 4), on the oceanic crust, several volcanoes have been identified. The onlapping seismic pattern associated with the first marine transgression suggests that they were active since the earliest stages of the generation of oceanic crust. However, timing of their extinction is less constrained and they might have been active at least until the Turonian. These volcanoes form a chain, named herein the Feilberg Volcanic Chain (Fig. 4), as it underlays the Valentin Feilberg Terrace, a distinct morphological sea floor feature (Hernández-Molina et al., 2009).

The Feilberg Volcanic Chain separates areas that experienced differences in accommodation. Landward of the chain the transgressive interval is relatively thin, whereas east of it, a much thicker interval has been deposited and preserved. As this feature evolved contemporaneously to the transgression, it might have controlled areas with restricted oceanic circulation from less restricted ones in an overall shallow sea. Morphologically it can be interpreted as an Outer High, analogous to Planke et al. (2000), limiting the SDRs as the youngest feeder system during normal breakup-. This feature is restricted to the segment between the Colorado Fracture Zone (CFZ) and the Bahía Blanca Fracture Zone (BFZ) (Fig. 4) and there some seismic evidences suggest that these volcanoes remained active long after oceanic crust was formed.

The Feilberg volcanic chain is also associated with a prominent magnetic anomaly, which has been recently modeled as the M7 anomaly. In view of its volcanic nature distinct from normal oceanic crust and its poorly constrained age, probably this interpretation deserves a revision (see section 6.1).

North of the BFZ up to the Tandil Fault Zone (TFZ) a number of smaller fracture zones have been interpreted, well developed on oceanic

crust, but also segmenting the SDRs. They form isolated pods during the early transgressive stages along a relatively narrower margin. Scattered volcanoes are associated to some of these fractures without significant offset. Fracture population is more prominent between the BFZ and the Ventana Fracture Zone (VFZ), the northern edge of Segment II *sensu* Franke et al. (2007).

Between the VFZ and the TFZ, bordering the Colorado Basin to the east, a small number of fracture zones have been recognized, suggesting continuous northwards propagation of the SDR feeder systems. The TFZ relates to a transtensional offset of the SDRs and south and northwards dipping magmatic packages.

North of the TFZ, some scattered fractures have been identified, probably more related to tensional gashes than accommodation during propagation.

The Salado Fracture Zone (SFZ) (Figs. 4 and 5) marks a prominent break of the SDRs, where transtension acted early on preserving deep depocenters related to the marine transgression. Fault activity seemed to have continued long after generation of oceanic crust. It is the northern limit of Segment III *sensu* Franke et al. (2007).

North of the SFZ along the eastern border of the Salado Basin again only minor fracturing is apparent. However, 3D seismic data show a complex network of fractures on top of the layers with highest impedance of the SDRs (Fig. 6).

The Rio de la Plata Fracture Zone (RPFZ) is distinct in several ways. Prominent fractures cut oblique across the SDRs and adjacent continental crust. There is a significant strike slip offset, as north of it oceanic crust is juxtaposed against continental crust to the south. This fracture might be a reactivation during breakup of a preexisting weakness zone (Fig. 4).

5.3. Barremian Aptian paleogeography of the Argentine margin

The emplacement of the SDRs and their segmentation created the framework in which the first marine transgression occurred. The early South Atlantic was highly compartmentalized with lows and highs restricting the oceanic circulation. Based on biostratigraphy Mc Millan (2003) suggests that seawater was hyposaline. In addition, the degassing associated to the emplacement of SDRs would have been erupted during a comparatively short interval might have contributed to increased CO₂ content, greenhouse climate and higher evaporation rates, which at a

global scale can be correlated with an Ocean Anoxic Event (OAE 1 b, Leckie et al., 2002).

The seismic record shows that transgression occurred stepwise, first flooding the fracture zones and then expanding on the previously exposed SDRs.

Fig. 7 shows a WNW-ESE oriented seismic line from the Salado Basin, covering the extent of the area flooded during the Barremian- Early Aptian. Assuming that the onlap to the SSW (right side) occurred on oceanic crust of Lower Aptian (M0) age, the half width of the Barremian South Atlantic did not exceed ≈ 200 km and the water depth remained overall shallow. Transgression started in the fracture-related depocenters and later onlapped on the SDRs. The smooth surface on top of the SDRs can be interpreted as evidence of erosion either subaerial or as a ravinement surface in very shallow water. At the eastern edge of the SDR wedge, a seismically more homogeneous feature resembles a plateau.

Towards the west, the extent of the first marine transgression is more difficult to outline. On some segments, a clear onlap pattern can be recognized, whereas in other areas, either lower accommodation prevented the accumulation of thicker deposits, or subsequent erosion affected the preservation of this section.

Fig. 8 is a dipline that shows differences between the top of the SDRs and the adjacent oceanic crust. While the top of the SDRs shows a smoothed surface, the oceanic crust is marked by a much rougher relief, probably the seismic expression of subaqueous episodic volcanism (seismic-scale equivalent of pillow lavas). The smooth surface at the top of the SDRs suggests processes of reworking, which can be the result of subaerial exposure before flooding and/or ravinement scouring during the earliest shallow-marine stages of transgression. In that case, it can be used as a proxy for the oldest coastline, against the SDR packages.

Interpretation of the seismic pattern suggests a stepwise transgression, punctuated by higher frequency stages of progradation. As marine transgression proceeded, preexisting drainage networks were flooded and constrained the areas of clastic supply into the sea. During high-frequency stages of progradation, either normal or forced small-scale deltas and laterally equivalent coastal systems developed, in most cases below seismic resolution. Fig. 9 shows a diagram illustrating the context of half-drowned SDRs, exposed along fractures. Erosion of those exposed edges resulted in local clastic coastlines. Towards the continent, longer lived fluvial systems eroded the nearby highlands. Tilting of the SDRs lead to restricted depocenters controlled by locally

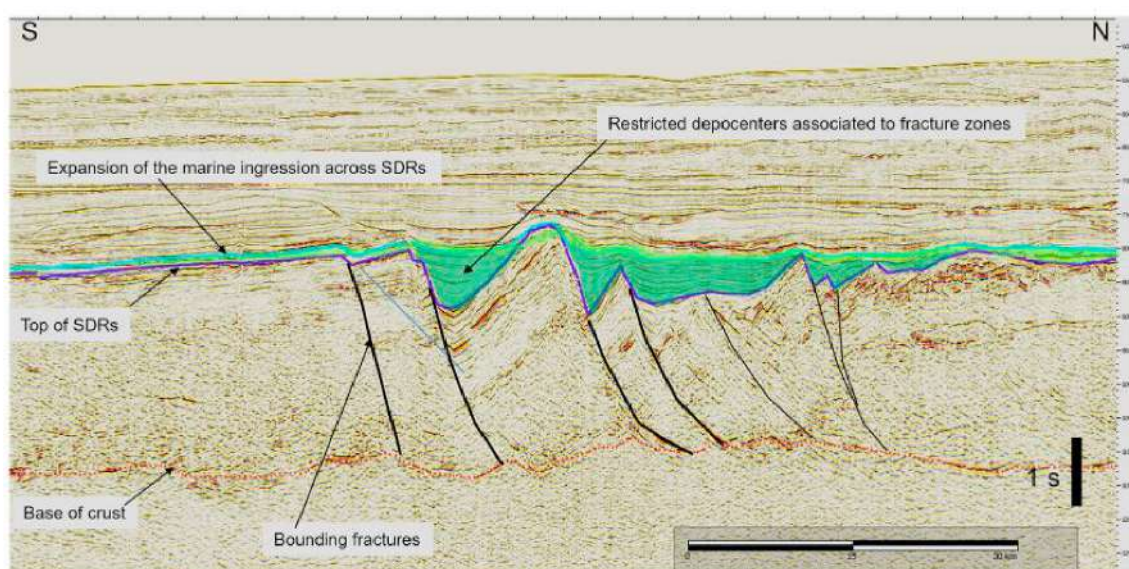


Fig. 5. Restricted early depocenters preserved in fracture zones segmenting the seaward dipping reflectors (SDRs). Fracture zones die out at the base of the crust. Restricted oceanic circulation within these fracture zones preceded expansion over the magmatic packages of the SDRs and oceanic crust. Salado Fracture Zone, strike line in the outer Salado Basin.

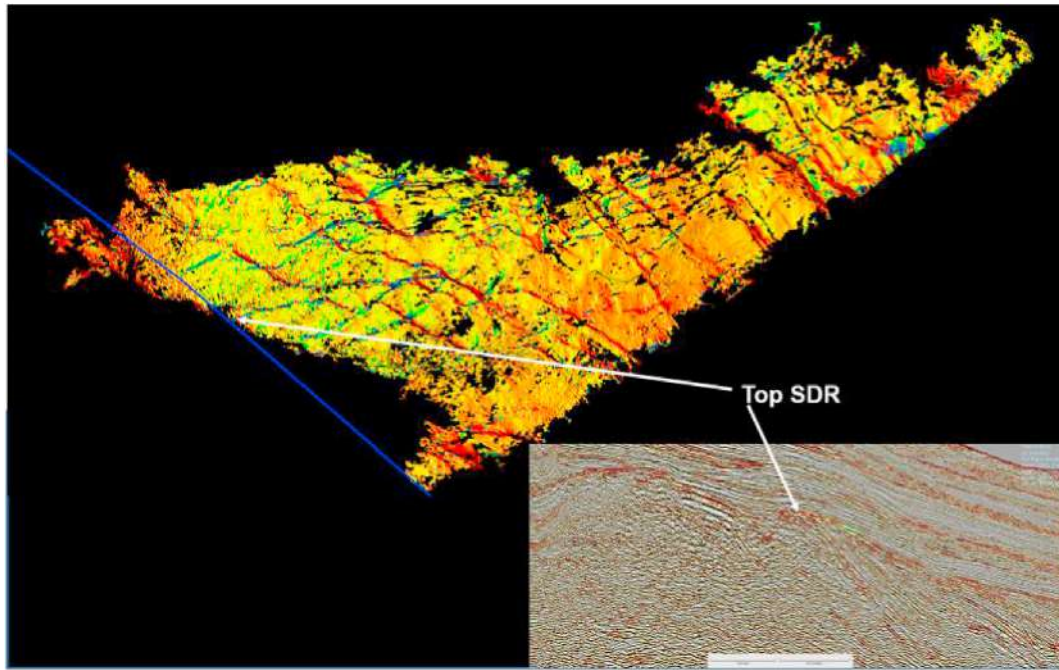


Fig. 6. SDR amplitude extraction with color coded azimuth changes showing a conjugate fracture network on top of a volcanic high impedance layer. The blue line indicates the inline position shown in the inset. Salado Punta del Este Basin, north of the Salado Fracture Zone. (For interpretation of the references to color in this figure legend, the reader is referred to the Web version of this article.)

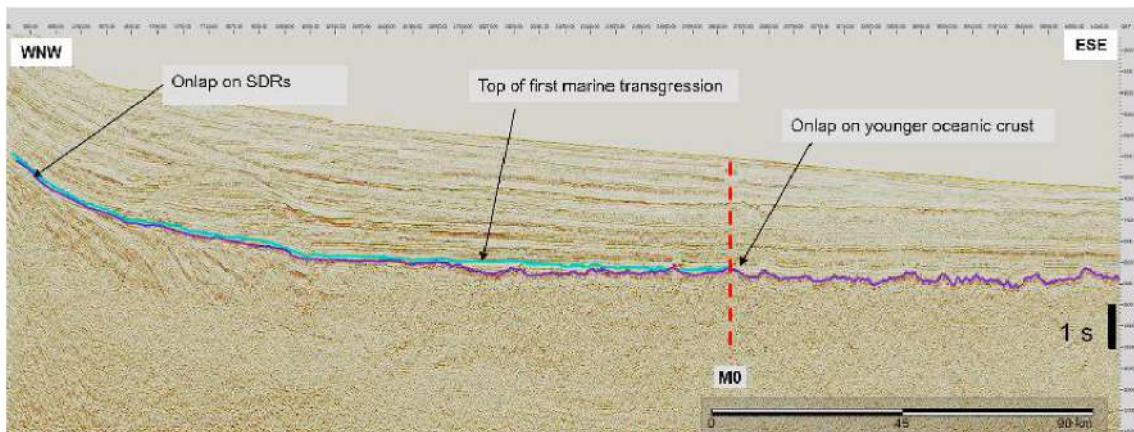


Fig. 7. Extent of the first marine transgression. The light blue marker is interpreted as the top of the first transgression, marking the base of the first progradation of Albian age. Towards the left (landward), the units onlap on the SDRs. On the right side (oceanward), the marker onlaps on oceanic crust younger than the M0 magnetic anomaly (projected as a red line). (For interpretation of the references to color in this figure legend, the reader is referred to the Web version of this article.)

acting thermal subsidence.

Where clastic supply was less prominent or the pace of transgression reduced the supply of clastic sediment to the sea, carbonate factories started to develop. Backstepping carbonates have been drilled in shallow waters in the Pelotas Basin further north and similar features have been interpreted between the Colorado Fracture and the Rio de la Plata fracture zones. In this area, for Barremian – lower Aptian times, global paleoclimate models suggest arid and warm conditions (Steinig et al., 2020 Dummann et al., 2020), still influenced by the welded Africa and South America landmasses. Locally, shallow SDR crests as well as flooded continental crust fractured by extensional tectonics conformed grounds for proliferation of carbonate factories. Final demise of carbonates was either related to increased bathymetry, higher clastic supply or change in environmental factors related to the evolution of the water body. Similar carbonates have been reported from the conjugate margin in the Orange Basin off Namibia and South Africa (Intawong

et al., 2019).

Fig. 10 illustrates a paleogeographic reconstruction of a carbonate factory. The model is based on data from the Salado – Punta del Este Basin, where the development of the carbonates is interpreted as having occurred on isolated basement highs inboard of the continent-ocean transition (COB). Rifting events predating crustal breakup generated a complex basement topography with highs and lows, which were successively flooded. Shallow areas, away from the clastic input points along the shore, were sites of emplacement of carbonate factories. The transgression led to a backstepping pattern of the carbonates. Also, in the Salado/Punta del Este Basin two growth stages have been recognized: an initial stage, somehow limited to the extent of the pre-existing high, and a second stage, where carbonate factories show a significant expansion beyond the initial structural boundary. The first step might be controlled by tectonic reactivations of the older extensional faults, whereas the second step marks the overall bathymetric control in

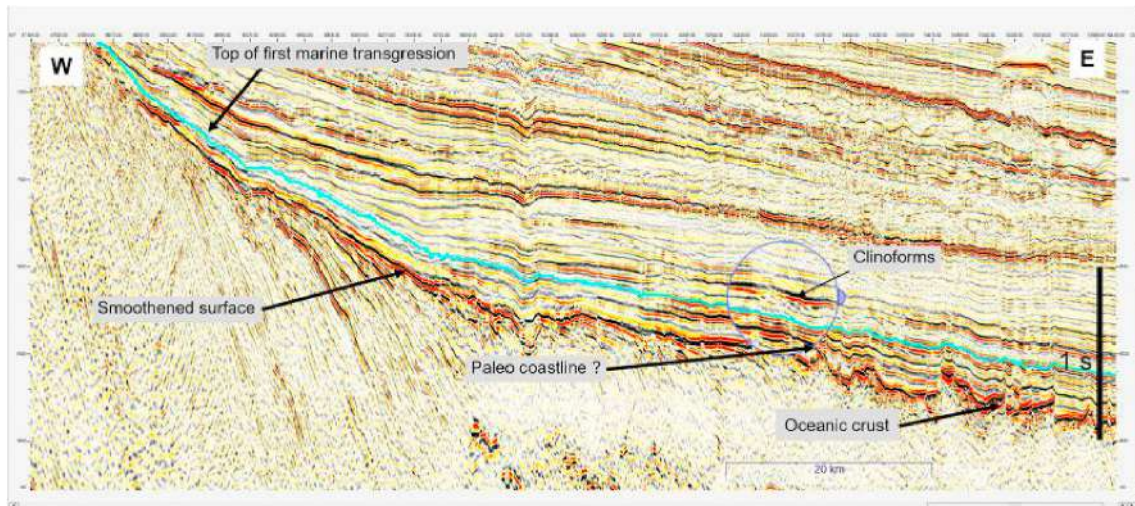


Fig. 8. Dipline showing the onlap of the first marine transgression, deepwater Colorado Basin. The smoothed surface on top of the SDRs contrasts with the roughed surface on top of the oceanic crust, separated from the SDRs by features that might correspond to the youngest feeder system of the SDRs. The zoomed inset (circle) shows the first clinoforms on top of the SDRs.

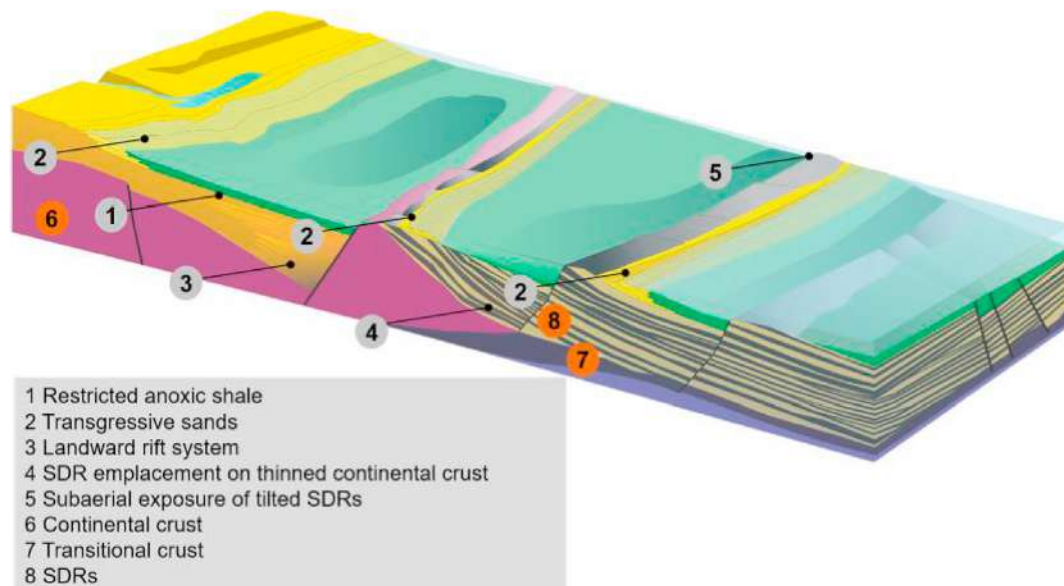


Fig. 9. Block diagram illustrating the depositional context of early clastic systems. Along the exposed crests of the SDRs erosion started to act and created sand strings filling restricted depocenters on the tilted magmatic packages. The shifting coastline was also marked by shallow-marine sandbars and deltaic systems from the drowned former fluvial network. Diagram not scaled, W to the left.

shallow waters. These two stages are separated by an irregular surface attributed to exposure and karstification.

In addition, the deeper areas surrounding the highs might have concentrated organic matter in an overall anoxic environment.

5.4. Connection between the Southern Sea and the early South Atlantic

Hofmann et al. (2014) analyzed the cores of the Albian – Aptian interval of DSDP wells 511, 327, 330 and 361. Around 112 M.a. a hiatus of 6 M.y. defined essentially by nannoplankton zonation seems to mark an erosive event, associated with a massive marine inflow into the South Atlantic across the Malvinas-Agulhas threshold.

The 112 M.a. timeline coincides with the maximum flooding marking the end of the Springhill transgression in the Austral and Malvinas Basins (Arbe, 2002). There, the event is marked by the extinction of the *Lenticulina nodosa* foraminiferal association, which can

also be identified in the Outeniqua and Orange basins (Brown et al., 1995; Mc Millan, 2003). This would be the first evidence of an effective marine connection of the southernmost South Atlantic with the Southern Sea. North of the Agulhas Malvinas fracture zone, on the South American side, no biostratigraphic data from wells for this interval are available. Therefore all interpretations rely on stratigraphic patterns, with loose ties to timelines.

The end of the transgression is marked by the earliest progradations, once the balance between accommodation and sedimentation changed in favor of the latter. This shift may have been caused by a decrease in the rate of relative sea-level rise or by an increase in siliciclastic sediment supply from the continent. Interpretation of the paleoenvironmental evolution of the first marine transgression can be summarized as follows.

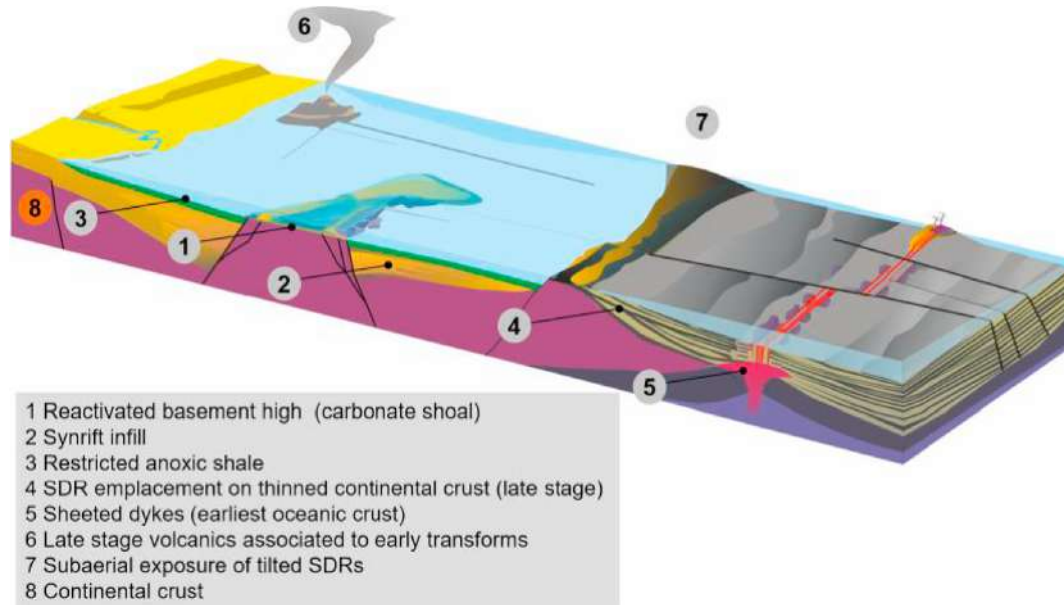


Fig. 10. Paleogeographic sketch of carbonate factories, offshore Salado Punta del Este Basin. At stages during which the clastic supply is outpaced by the rate of transgression, in shallow areas related to basement highs inherited from previous rifting, carbonate factories develop, recording stages of sea level oscillation during the Barremian Aptian transgression. The paleotopography controlling the carbonate factory emplacement constrains oceanic circulation and might favor anoxic shale deposits. This reconstruction from the Salado Punta del Este Basin assumes subaerial exposure of SDRs by tilting and later flooding. Diagram not scaled, W to the left.

5.5. Summary and discussion - the first marine transgression

After the onset of magmatic activity controlled by fractures aligned with the future continent-ocean transition zone (COT), a highly segmented basinal area developed. Primitive connection between the Southern Sea and the embryonal South Atlantic occurred north of the Malvinas platform, following transtension and rifting south of the Outeniqua Basin. The fracture zones, which separate the segments along

which breakup propagated towards the north, initially generated areas with increased crustal thinning and magmatic feeding. Cooling afterwards promoted accommodation creating ponded areas, with restricted circulation and anoxic environment.

The SDRs were emplaced subaerially and later reworked by waves in shallow waters during subsequent transgression (ravinement erosion). Where existing networks transferred clastic supply into the basin, transgressive sandstones developed as backstepping shorelines, fringing

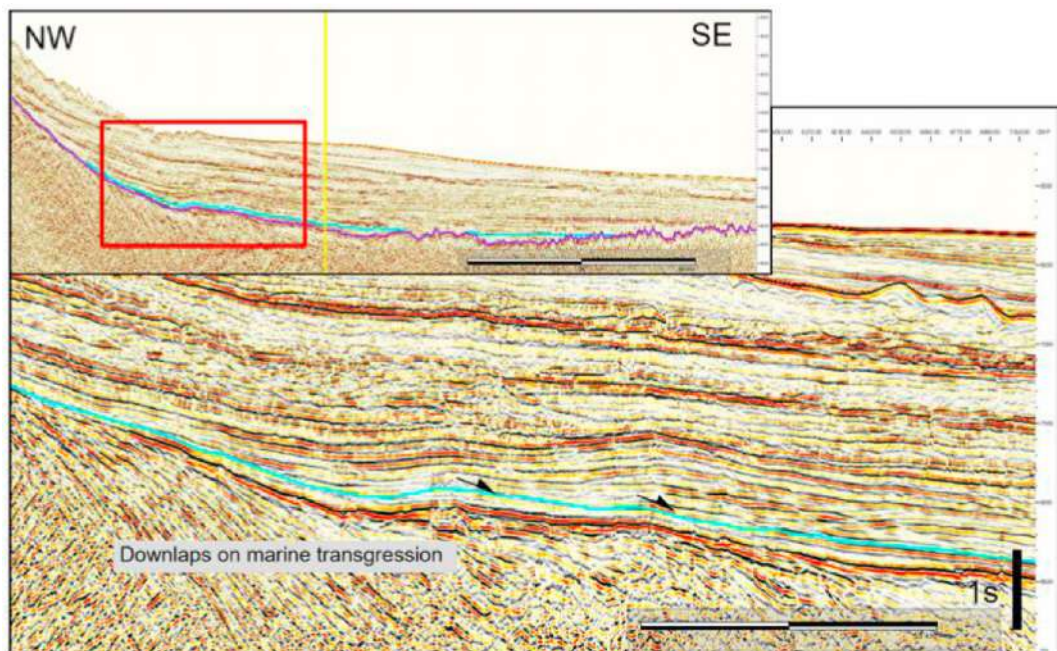


Fig. 11. Diapline showing the extent of the first transgression (light blue) and on top downlapping clinoforms related to the first progradational cycle. These progradations mark the diachronous boundary where sediment supply overpassed the rate of accommodation. The onset of progradations occurred earlier in a landward direction, relative to these features observed down-dip. The overall geometry assumes a shallow marine ramp setting. Blue marker represents the top of the first marine transgression. Inset shows location of zoomed area. (For interpretation of the references to color in this figure legend, the reader is referred to the Web version of this article.)

exposed shoulders of the tilted SDRs.

As thermal subsidence continued, tilting of the SDRs became more severe while the spreading center became more distant to the COT; as a result, they started to subside and were onlapped by marine deposits.

Transgression operated in high-frequency pulses. Sediment supply to the sea likely increased during the regressive phases of these high-frequency cycles. Areas of lower sediment supply afforded the development of shallower water carbonates, which described a backstepping stacking pattern during the long-term transgression.

6. Progradations into a shallow sea

The first marine transgression occurred stepwise. When the rate of accommodation was outpaced by clastic input, the first progradation of the passive margin began and a depositional shelf break developed. During the early stages of the transgression, clastic input may have generated a veneer of backstepping shorelines below the seismic resolution. Accommodation continued to increase subsequent to the initial transgression of the passive margin, allowing the formation and preservation of the clinoforms seen on top of the maximum flooding surface (Fig. 11; Helland Hansen et al., 2012).

The hinterland was probably dominated by low ranges related to the eroded remnants of cratons (Deseado craton, Rio de la Plata craton, Australes fold and thrust belt, etc). Given the thermal-driven subsidence along the rift system inherited from previous extensional strain at high angle to the continent-ocean transition (COT), it is likely that the oldest sediment dispersal systems followed the axes of the Colorado and Salado Basins. To date, clastic supply areas are not well constrained, but Apatite Fission Track Analysis (AFTA) data indicate that both the Paleozoic fold and thrust belt of the Sierras Australes, north of the Colorado Basin and the Tandilia Basement High, were uplifted since Jurassic times, predating the breakup (Kollenz et al., 2015). Eventually, during the uppermost Cretaceous, when the Neuquén Basin turned into a foreland, coincident with overfilled stages, sediment might have been transferred from the Neuquén Basin to the Colorado Basin, through a complex paleo-fluvial network.

6.1. The earliest shelf break

The oldest prograding systems were probably deltas built out in shallow waters, likely to be below seismic resolution on the thin transgressive layer later tilted to the east. The outline of the oldest shelf break along strike involves a series of diachronous clinoforms, whose identification (i.e., scales above or below the seismic resolution) depends on the rates of clastic supply, which vary according to the location of the feeder systems, and their preservation during the instability that accompanied the subsequent deepening of the basin. In deep water, the bottomsets associated with these clinoforms can only be differentiated from the flat lying transgressive strata below, by lateral changes in amplitude.

Fig. 11 is a dipline that shows the boundaries of the first transgression in the deep-water setting of the Salado Basin. Above the SDRs a series of parallel reflectors can be recognized that onlap to the left side (West) of the section. On top of it overlapping reflectors mark the advancing base of the prograding slope.

Fig. 12 represents a paleogeographic outline for the time interval postdating the first transgression. Time constraints can be obtained only from the conjugate African margin, taking into account the diachroneity from south to north.

Climoforms related to a stratigraphic (depositional) shelf break have been identified at several locations, from the Colorado Fracture Zone (CFZ) to the Salado – Punta del Este Basin. They are well preserved due north of the CFZ (Fig. 13) and in the Colorado Basin embayment, although in the latter location, erosion of the slope cut deep into the shelf edge and disconnected bottomsets off the slope from the clinoform rollovers further landward. Connectivity between the clinoforms and the

bottomsets is well preserved in the Salado-Punta del Este Basin, in particular north of the Martín García High, where a wide embayment developed (Fig. 12).

The first regression is assumed to have occurred after the maximum flooding of the Aptian (113 M.a.). The width of the shelf was variable. In the Colorado Basin the width of the shelf between the youngest onlap on the underlying basement and the edge at the end of progradation did not exceed a few tens of kilometers. North of the Colorado Basin, the shelf only developed as a narrow fringe that was later eroded. In the Salado – Punta del Este Basin however, it followed a sharp turn to the northwest, along the northern flank of the Martín García High, opening to a broad embayment that extended into the southern Pelotas Basin, outside the area studied.

Within the study area, shelf edge trajectories could be determined south of the Colorado Basin (Figs. 13 and 14, see below).

Between the CFZ and the Agulhas-Malvinas Fracture Zone, no clinoforms could be identified, only an interval of parallel reflections whose seismic facies differs from the transgressive section below. While the transgressive interval is characterized by a more transparent section, the interval on top of the maximum flooding surface is marked by laterally continuous reflections. The latter interval may be the bottomset of clinoforms located farther updip.

Current seismic resolution does not allow identification of transform faults separating segments dominated by extensional faulting. What is apparent in this segment (between the AMFZ and CFZ) is a much steeper margin, where a sudden increase in water depth precluded the development of a shelf break and instead sediments were transferred directly into deep water with little selection mechanisms.

6.2. A narrow shelf and progradations into a shallow sea

With the current database it is not possible to determine the age of the clinoforms north of the CFZ. However, the detailed sequence stratigraphic analysis carried out by Brown et al. (1995) shows some common patterns between both margins. Also, the biostratigraphic framework of Mc Millan (2003) yields additional time constraints. In particular, in the Orange Basin, they recognized two progradational cycles above the first transgressive interval (13At1) and bounded at the top by an unconformity (14At1), followed by a third progradational cycle. The top of this interval is marked by a regional unconformity labeled 15At1, which has been dated as Cenomanian-Turonian boundary. At its current state it is difficult to correlate all the lower rank sequences defined in the Orange basin with their likely South American equivalents, but at least until the Cenomanian-Turonian boundary there are strong similarities in their stratigraphic pattern.

Along the southern South American margin, an equivalent interval is best represented in the area of the Colorado Basin. Figs. 13 and 14 show a dip line where the oldest progradational system has been defined south of the Colorado Basin. At the base of the overlapping clinoforms a blue marker, interpreted as the top of the previous transgression, can be seen. The top of this interval is marked by a regional unconformity of tectonic origin (see section 7).

The Barremian-Aptian transgression created the space for the first normal regressive clinoforms interpreted as the first highstand of the basin. The distance between the onlap on the basement and the shelf break is in the order of a few tens of kilometers, which suggests a relatively narrow shelf. The bottomsets associated to this highstand are difficult to separate from the underlying transgression, whereas the top of this systems tract is eroded by processes associated with the following fall in relative sea level. The offlapping clinoform rollovers mark the location of the shoreline at the shelf edge during the forced regressions. Basinward, some chaotic reflectors might be interpreted as base-of-slope gravity flows, either grainflows or high-density turbidites. The end of the forced regression is marked by the onset of upstepping of the clinoform rollovers and the accumulation of topset deposits of the following lowstand systems tract. The onset of transgression is

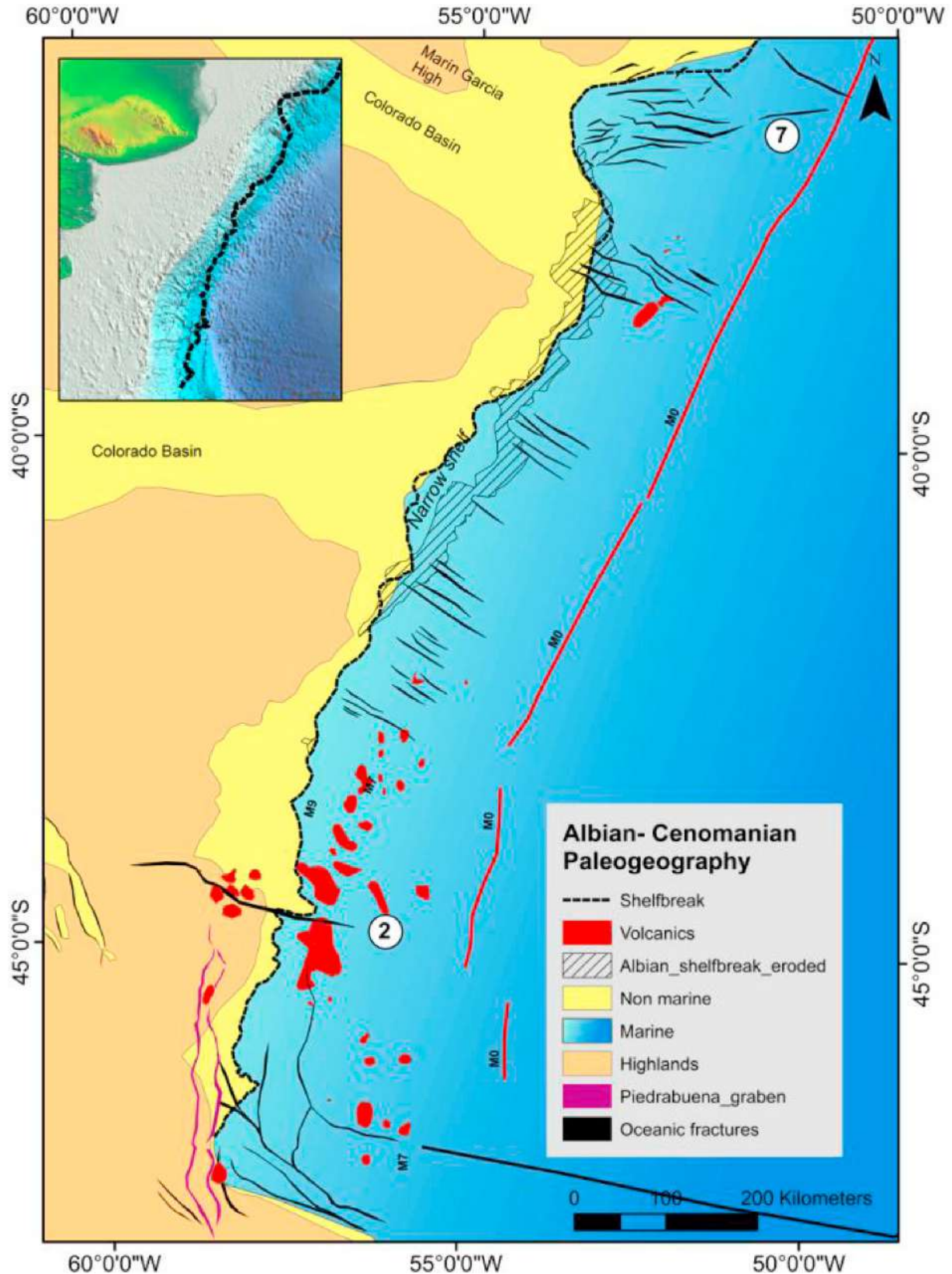


Fig. 12. Paleogeographic outline for Albian-Cenomanian times. The area of non-marine sedimentation is located updip from the points of offlap or coastal onlap. Shelf break progradations have been identified between the Colorado Fracture Zone (2) and the Rio de la Plata Fracture Zone (7). Post Albian uplift eroded part of the shelf break and adjacent bottomsets (hatched areas). Where preserved, at least two progradational cycles could be defined, best developed south of the Colorado Basin. Red line is the M0 anomaly for paleogeographic comparison with Fig. 4. (For interpretation of the references to color in this figure legend, the reader is referred to the Web version of this article.)

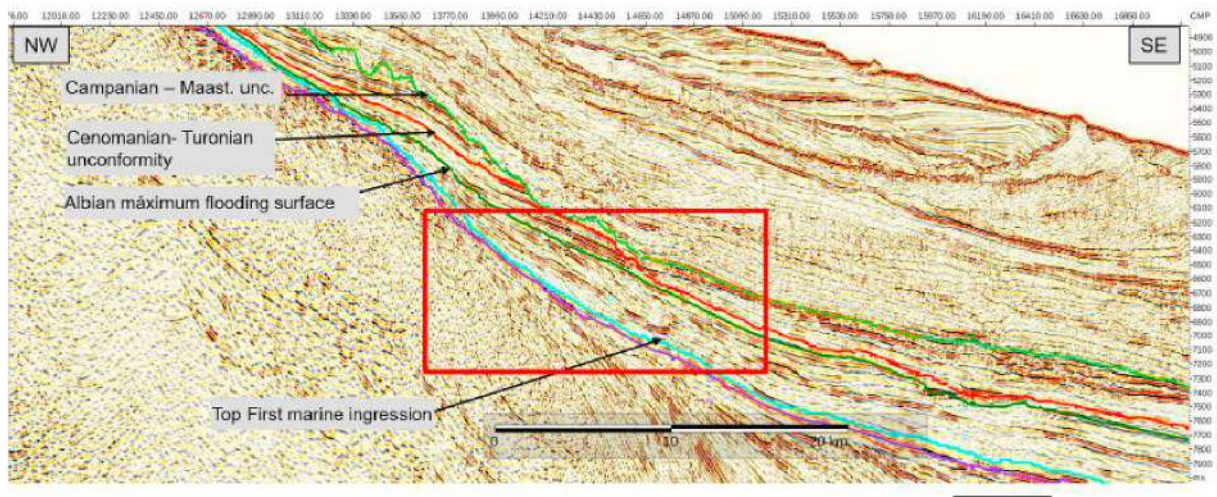


Fig. 13. Clinoform sets developed on top of the first transgression south of the Colorado Fracture Zone. The blue marker indicates the top of the sediments accumulated during the transgression, while the accommodation for the prograding clinoforms was created. Seismic line in TWT, but interval velocities support stratigraphic shelf clinoforms according to water depths of c. 250–300 m. See text for further explanations. Inset indicates zoomed and flattened section, shown on Fig. 14. Vertical scale to the left is in milliseconds. (For interpretation of the references to color in this figure legend, the reader is referred to the Web version of this article.)

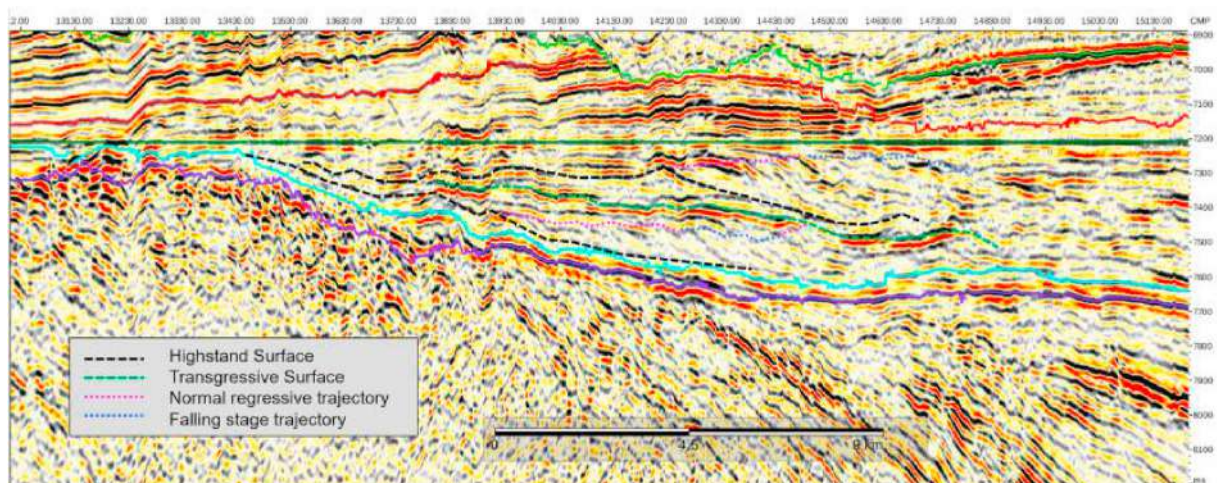


Fig. 14. Section (inset on Fig. 13) flattened at the maximum flooding surface (Upper Cenomanian) on top of the two packages of clinoforms. The blue–red lines mark the shelf edge trajectory during the progradation of the clinoforms, with the blue segments corresponding to normal regressions (progradation and upstepping) and the red ones to forced regressions (progradation with downstepping). The first blue segment may be interpreted as the highstand that follows the first marine transgression, whereas the second blue segment, which follows forced regression, as a lowstand normal regression. The transgressive deposits are significantly thinner than the regressive deposits, which form the bulk of the succession. The dip angle of the forced regressive clinoforms, assuming an interval velocity of 2400 m/s, is in the order of 6–8°. Vertical scale to the right is in milliseconds. (For interpretation of the references to color in this figure legend, the reader is referred to the Web version of this article.)

associated with chaotic features that can be interpreted as slumps on the slope. Above the maximum flooding surface, the highstand systems tract is poorly represented at the seismic scale, before the start of the next fall in relative sea level and the associated falling-stage systems tract.

The second cycle bears similar features with the first one, starting with forced regression that changed into lowstand normal regression. During the falling stage landward of the clinoform rollovers, some erosive features were identified, likely to correspond to fluvial incised valleys. Basinward, an erosive surface extends into the deep water, suggesting erosion by mudflows, which could be followed by turbidites. Topsets deposited during the normal regression of the lowstand are better preserved and indicate less sediment transfer across the shelf to the deep-water setting. The transgression is marked by onlap on the shelf and a shift of the coastline to the west. The highstand systems tract is

eroded by what has been interpreted as a second-order unconformity related to the change in the plate-tectonics configuration of the South Atlantic at the Cenomanian-Turonian boundary.

The two prograding cycles show an overall narrow shelf, where the coastline reached the shelf edge during forced regressions. This favored an efficient sediment transfer across the shelf to the slope. An increase in slope gradient during forced regressions suggests coarser grained flows such as grainflows, whereas decreasing clinoform angles could indicate the accumulation of high- to low-density turbidites. If the height of the clinoforms can be regarded as a proxy of the paleo-water depth, the toe of the slope was located at minimum 250–300 m below the sea level.

Fig. 14 shows a detail of the same line flattened to the maximum flooding surface which marks the end of the first two progradational cycles. The blue and red markers show the shelf edge trajectory, where

forced regressions alternate with stages of normal regression.

The initial geometry of the margin seems to follow an overall ramp-like setting, from the continental crust to the young oceanic spreading ridge. Based on an average interval velocity, the height of the clinoforms is in the order of 240 m, which approximates the paleo-water depth. The slope angle of 8° is within the range of worldwide known orders of magnitude, although on the steeper end. The scale of the clinoforms allows us to conclude that until the end of the Cenomanian, the sea that transgressed the young passive margin was relatively shallow.

The connection between the clinoforms and bottomsets off the slope is preserved in the south and northernmost part of the margin, but in between most of the lower slope has been eroded (diagonally ruled in Fig. 12) by the Cenomanian-Turonian unconformity (see next section).

Fig. 15 is a sketch of the Albian - Cenomanian paleogeography. According to what can be observed on the seismic data, the youngest volcanoes associated to fractures feeding the magmatic packages of the SDRs were active at least until Cenomanian times. The geoseismic section shown on Fig. 17 marks the unconformity between the Albian-Cenomanian and Turonian-lower Campanian interval. The unconformity onlaps on Feilberg Volcanic Chain. Therefore this feature initially acting as the feeder for the youngest SDRs, persisted after the generation of oceanic crust. The meaning of the magnetic anomaly and its age, associated with this feature should therefore taken with care.

Fig. 16 is a zoom highlighting the depositional processes associated with the earliest clinoforms. The shoreline shown on the map possibly underestimates the extent of the sea, as it is likely that initially shoreline deposits as well as deltaic systems developed at scales below seismic resolution. However, the onlap of this section on the exposed clastic source areas gives a true control on the sedimentary extent of the unit. Concomitant with the progradation, a stratigraphic shelf break developed. The width of the shelf could only be defined in the Colorado Basin. There, 3D data allow identification of both the coastline as well as the shelf break by seismic geomorphology interpretation from RMS amplitude extractions. As such, the width of the shelf was in the order of 40 km. The reduced width promoted the full exposure of the shelf during forced regressions and the development of shelf edge deltas albeit likely below seismic resolution. In some cases, transgressions fill and preserve incised valleys cut into the underlying topsets of the normal regression stages.

Along the northern edge of the Martín García High that separates two graben systems in the Salado-Punta del Este Basin, a higher shelf break

(i.e., larger scale clinoforms) developed. Supply to the shoreline is controlled by the Martín García High and the Highlands NE of it. Unlike the segment south of the Martín García until the Colorado Fracture Zone, accommodation is controlled by NW-SE oriented transtensional faults.

This additional accommodation mechanism promotes the development of steeper clinoforms, similar to the model for a combined stratigraphic-structural shelf (Helland Hansen et al., 2012). In this context, the Martín García High remained exposed and a clastic source area until the end of the Cretaceous.

The maximum flooding surface at the top of the progradational cycles is preceded by slumping of the slope, probably due to instability during the transgression. In deep water, this erosional surface can be followed as a prominent marker but only on some segments it is clearly connected to the shelf edge. This maximum flooding surface is marked by an aggradational-backstepping pattern, barely above seismic resolution.

The paleoenvironmental interpretation outlined above affords a series of conclusions, as summarized below.

6.3. Summary and discussion –shallow marine deposition

The Barremian – Aptian transgression occurred in a ramp-like setting. The ramp geometry developed on top of the basement and the adjacent SDRs, inherited from the previous stage, and favored the development of a stratigraphically controlled shelf-slope system. The shelf was rather narrow in the order of 40 km, with efficient transfer of riverborne sediment to the growing slope. At least two prograding cycles have been defined, separated by a maximum flooding surface of a lower hierarchical rank. The height of the clinoforms is in the order of 300 m, which indicates a relatively shallow water depth. Variations in the relative sea level are recorded by changes in stratal stacking patterns on the shelf. In the seismic record, a clear alternance between normal and forced regressions can be observed, where the stages of forced regression resulted in shelf exposure and maximum migration of the coastline to the shelf break. Fluvial topsets alternate with incised valleys on a short distance and likely within a short timeframe. The depositional processes that dominate the slope are essentially gravity flows. Erosion of topsets accumulated during normal regression, as well as the bypass of the shelf during forced regressions, resulted in high sediment supply to the slope, generating steep clinoform surfaces with a higher angle of stability as it is typical for sand-rich gravity flows (e.g., grainflows and high-density

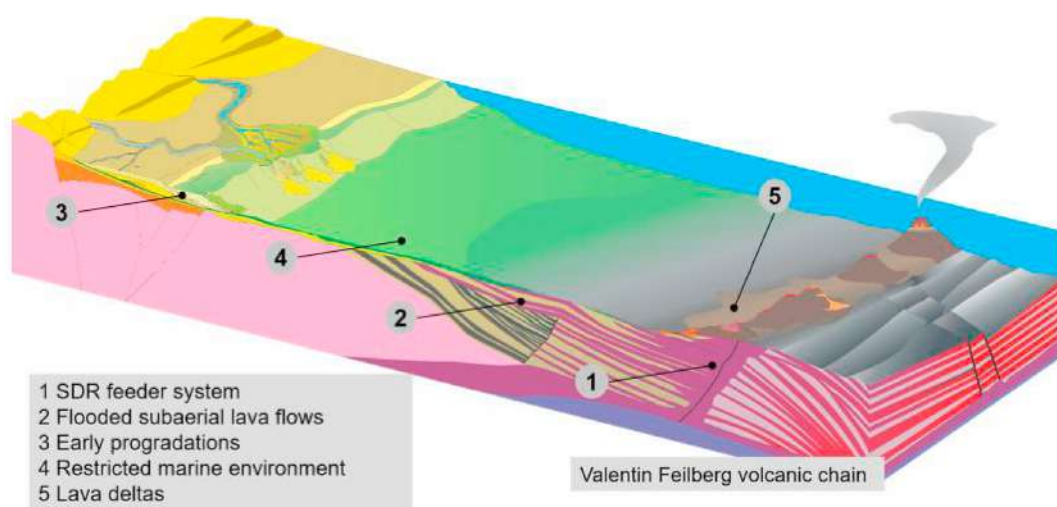


Fig. 15. Sketch showing a reconstruction of the Albian-Cenomanian shelf-slope system, south of the CFZ, based on the seismic interpretation shown in Figs. 13 and 14. The Barremian-Aptian transgression is followed by a highstand during which a narrow stratigraphic shelf developed (see Fig. 16 for details). Offshore, the emplacement of magmatic packages remained active along the volcanic chain (Valentin Feilberg chain). After the first stages marked by subaerial flow of significant lateral extent, during marine transgression and the following highstand, lava deltas developed around the volcanoes active along the magmatic feeder fractures. Not to scale, landward (west) is to the left.

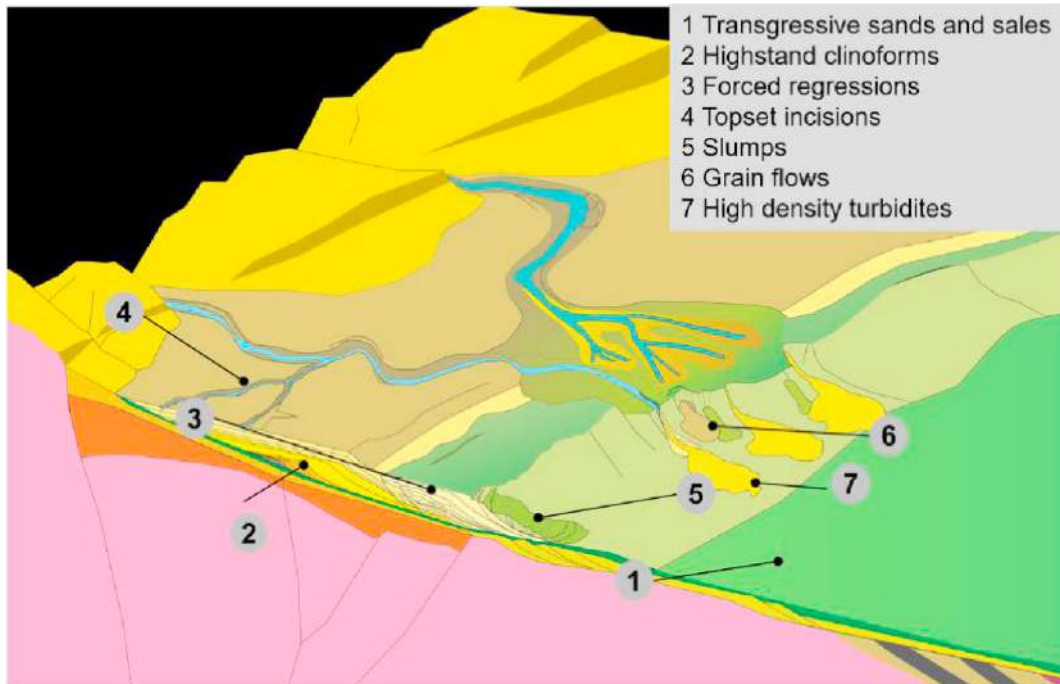


Fig. 16. a: Zoom of the Albian-Cenomanian shelf-slope system, showing the evolution of the different systems tracts. After the first transgression was outpaced by clastic supply, a highstand wedge building up a narrow shelf developed. Lowering of the relative sea level resulted in exposure of the shelf and incision along the fluvial systems concomitant with the development of forced regressions. Lowering of the wave base resulted in shelf edge instability and removal of sediments and transport across the shelf. The first stages were characterized by slumps followed by grainflow deposits and high-density turbidites, in particular close to the shelf edge deltas as rivers moved across the shelf.

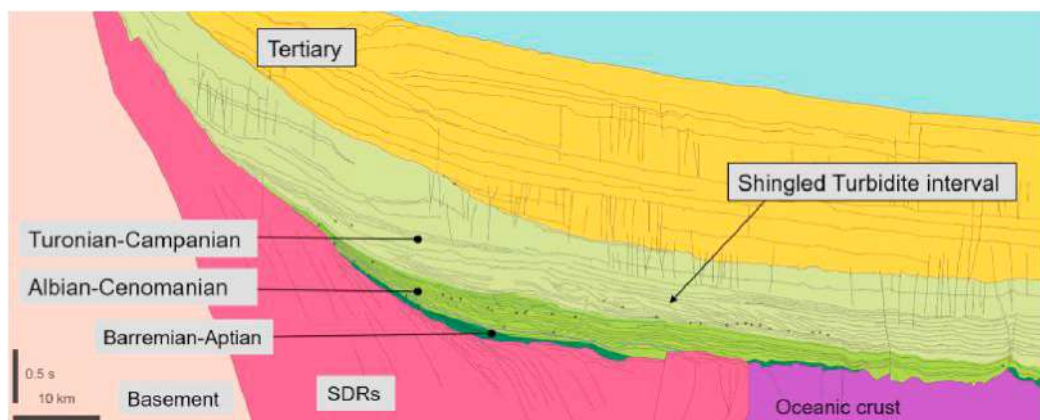


Fig. 17. Geoseismic cross section between the outer Salado and Colorado basins, where the shingled turbidites are best represented. The base of the shingled turbidites represents the onset of bathymetric change from a shallow (250+ m deep) marine environment to a deep marine environment, with well-developed canyon slope, systems interacting with thermohaline currents and basin floor fans towards the basin plain.

turbidites). In the late stages of forced regressions, base of slope fans are most likely to develop, upstream connected to incised feeder systems. The maximum flooding surface on top of the two cycles is followed by a section of concordant parallel reflectors, poorly preserved as they have been eroded by the Upper Cenomanian – lower Turonian unconformity (section 7). During this stage, the Feilberg Volcanic Chain created a topographic segmentation creating a barrier for the sediments transported across the slope into open waters.

7. Increased subsidence and development of a tectonically driven shelf break

The major transgression that followed the two cycles described in the previous section is truncated by the Upper Cenomanian-Turonian

unconformity (age interpretation tentative). This unconformity is a second-order boundary within the first-order passive margin sequence, as it is not constrained to a particular basin but rather can be followed along the whole margin.

A time equivalent unconformity is recorded in the Orange Basin and it is interpreted as a readjustment of the margin, as the two continents, i. e. South America and Africa, finally break free between the Malvinas platform and the SW edge of Africa (15 At1 unconformity in Brown et al., 1995).

The separation between South America and Africa resulted not only in a higher spreading rate but also in a flexural adjustment of the margins and accelerated cooling of the crust. Cooling favored an increase not only in the accommodation rate, and the associated increase in bathymetry that led to the Cenomanian transgression, but also changed the

gradient of the seafloor. Flexural adjustment of the margin resulted in exposure and erosion of the Albian shelf deposits and constrained the initial geometry for a structurally controlled shelf break in the sense of Helland-Hansen et al. (2012).

7.1. A change in shelf-break geometry

The top of the first shallow-marine clinoform interval interpreted as of Albian to Cenomanian age is eroded by a regional unconformity that cuts into the shelf edge. It can be followed into deep water where along certain segments of the margin it marks the base of a series of oceanward dipping reflectors as “shingles”. Based on their expected depositional environment they are regarded as prograding deep water turbidites, following an increase in the gradient of the basin floor.

The uplift resulted in the exposure and erosion of the shelf, which is most prominent outside the basinal areas of the Colorado and Salado basins where additional subsidence compensated part of the regional uplift. At the same time, increased cooling of the oceanic crust steepened the sea floor, promoting transport of sediments and even a frontal stacking conforming a shingled array of turbidites. This feature is interpreted as a key to the definition of the correlative surface of the regional unconformity that eroded the shelf and coastal areas, when continents began to completely separate from each other.

Between the Salado and Colorado basins, several high-amplitude reflectors resemble intrusive bodies. They might be associated to magmatic bodies that followed a fracture network developed during the flexure of the margin.

The flexural deformation on the shelf was followed by a readjustment marked by a transgression assumed as of mid-Turonian age. Resumed sedimentation copies the geometry inherited from the erosion and delineates a structurally controlled shelf break, and a larger scale (i. e., deeper) slope.

Fig. 17 shows a geoseismic cross section where the shingled turbidites are well represented on top of the Albian – Cenomanian clinoforms. The surface at the base of the shingled turbidite complex is interpreted to mark the change in seafloor gradient due to increased cooling rates, which promoted a longer transport distance off the toe of the paleoslope. Given the uncertainty in age inherent to this interpretation, the transgressive interval on top of the shingled turbidite interval could be correlated with the early Turonian transgression, followed by the mid Turonian unconformity which marks the onset of deep-water turbidites.

7.2. An open marine shelf and slope with higher accommodation

Fig. 18 shows a paleogeographic outline representative of the time interval (Upper Cenomanian–Turonian) shortly after the structural shelf break and slope came into being. The shelf is still rather narrow, according to a few control points where deltaic clinoforms at nearly sub-seismic scale could be identified. Most sediment supply follows the inherited basin axis (namely Colorado and Salado basins), where the depositional pattern is best preserved.

In the Salado – Punta del Este Basin, the shelf break is well preserved, as part of a sedimentary wedge fed by the combined sediment supply from the Martín García High to the west and the basement exposed to the north. Along the southern Salado Basin and the Tandilia High, the shelf edge has been partially eroded by the Campanian–Maastrichtian unconformity (see section 6.1). At the outer edge of the Colorado Basin, the shelf break is well preserved, due to a combination of increased subsidence and sediment supply along the basin axis.

South of the Colorado Fracture zone, the shelf break is very narrow. A shelf break with well developed (i.e., at seismic resolution) clinoforms is largely related to margin segments where onshore fluvial systems develop broad catchment areas, concentrating sediment within delta systems, with further sediment transfer across the shelf. Smaller rivers with reduced catchment areas would not be able to create deltas and shelf clinoforms, but rather fan deltas of reduced extent, below seismic

resolution. Thus, the coast south of the Colorado Fracture Zone during Cenomanian – Campanian times can be interpreted as dominated by nearby highlands (the Deseado massif) with short fluvial systems without significant transport capacity or sediment concentration on the shelf.

According to Holmes et al. (2015) in the North Malvinas Basin the first marine transgression occurs after a regional unconformity which truncates the Late Valanginian to Cenomanian fluvio-lacustrine rift infill.

The sequence stratigraphic framework of the Cenomanian – Campanian interval can be best imaged in the outer Colorado Basin. Fig. 19 a and b are uninterpreted and interpreted dielines of the Colorado Basin showing the clinoforms developed during this stage. The lowermost two clinoform cycles are regarded as time equivalents to the Albian clinoforms defined further south and shown on Figs. 13 and 14. Although it is likely that both accommodation and supply vary along strike, the main two-cycle pattern (i.e., highstand normal regression followed by a falling-stage with forced regressions, followed in turn by lowstand normal regression) can be identified. The second regressive stage is followed by a transgression that led to a significant landward relocation of the highstand clinoforms. The top of these cycles is marked by the Upper Cenomanian–Lower Turonian unconformity. At this location, the unconformity relates to significant slope instability with slumping and sliding and even wedges showing internal thrusting, indicative of a change in the gradient of the seafloor.

On top of this unconformity, a thin transgressive section, probably preceding the Middle Turonian highstand, developed. It is followed by low angle clinoforms, indicative of a fast progradation likely related to increasing sediment supply. They have been interpreted as highstand systems tract, assuming that the lowstand on top of the unconformity was not preserved by erosion acting along the slope. Towards the left (west) cut-and-fill geometries could be interpreted as corresponding to fluvial sediments of the highstand topset.

These topsets have been eroded during the next falling stage, when the pre-existing shelf is eroded and locally shows collapse features. This collapse controlled the next falling-stage system tract, which healed this feature. On top of some chaotic reflectors, interpreted as slumps, downlapping clinoforms prograded during the falling stage. These clinoforms show comparatively steep angles of repose, suggesting deposits with coarser grain size. Once the shelf collapse was healed, progradations with an aggradational pattern and topset development defined a lowstand systems tract. Landward of the shelf break, an erosive surface cutting across relatively thin transgressive deposits is apparent, likely to be a ravinement surface linking the onset of transgression with the maximum flooding surface. On top of this transgressive interval, low angle clinoforms are indicative of resuming clastic influx and fast progradation. Their increase in height suggests also an increase in accommodation across the shelf and slope. These clinoforms are truncated by the next falling stage, when the oversteepening of the slope led to slumping and sliding.

The whole interval is truncated by a strongly diachronous (Campanian–Maastrichtian) regional unconformity which will be discussed in Section 6.

7.3. Deep marine slope deposition

While the shelf recorded the changes described above, gravity flows on the slope led to sediment transport extending away from the toe of slope onto the basin floor. Initially mudflows and slumps eroded the seafloor forming slope canyons, which later became the conduits for sand-rich turbidite flows that built out basin floor fans. Over time, sediment feeder systems developed across the shelf during the falling stages stayed active even during highstands, resulting in a complex vertical stacking of alternating high- and low-density turbidites, inter-laced with mudflows. In deep water, depending on the supply rate, basin-floor fans developed. In addition, the increased water depth and

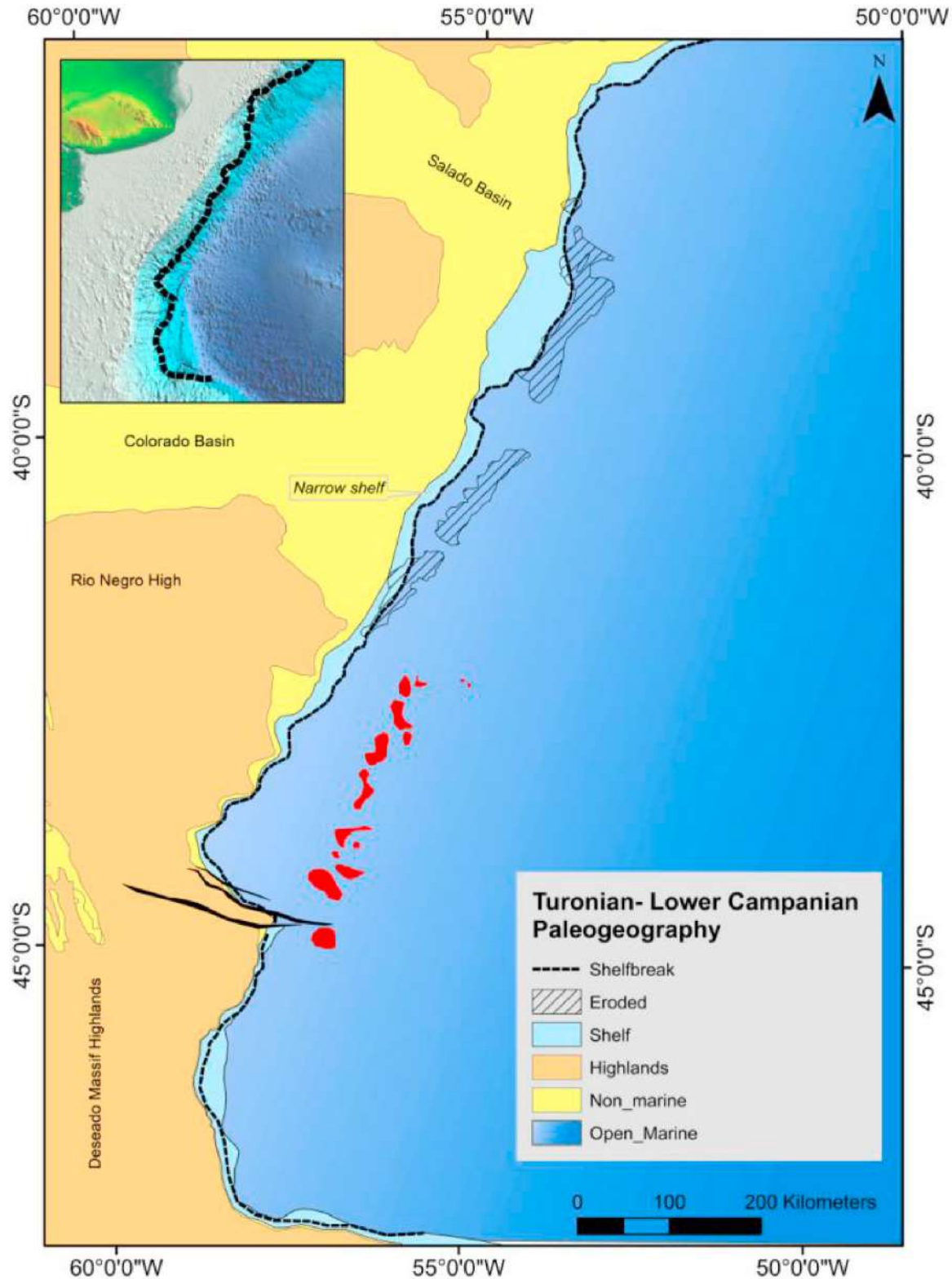


Fig. 18. Turonian- Lower Campanian paleogeography. After the Upper Cenomanian/- Lower Turonian unconformity, a structurally enhanced shelfbreak developed, as a consequence of increased spreading rates combined with flexural uplift of the margin. For the first time, slope channels appear in the stratigraphic record of the margin, indicative of a broader shelf and a longer slope, which also accounts for basin floor fans off the base of slope. Erosion or no deposition on the shelf indicates that there is significant bypass and transfer of sediment into deep water. Well developed canyon systems have been defined between the Colorado Fracture (2) and the Rio de la Plata fracture zones (7). South of the Colorado Fracture Zone, a narrow shelf developed, bordering what is interpreted as the Deseado Massif Highland.

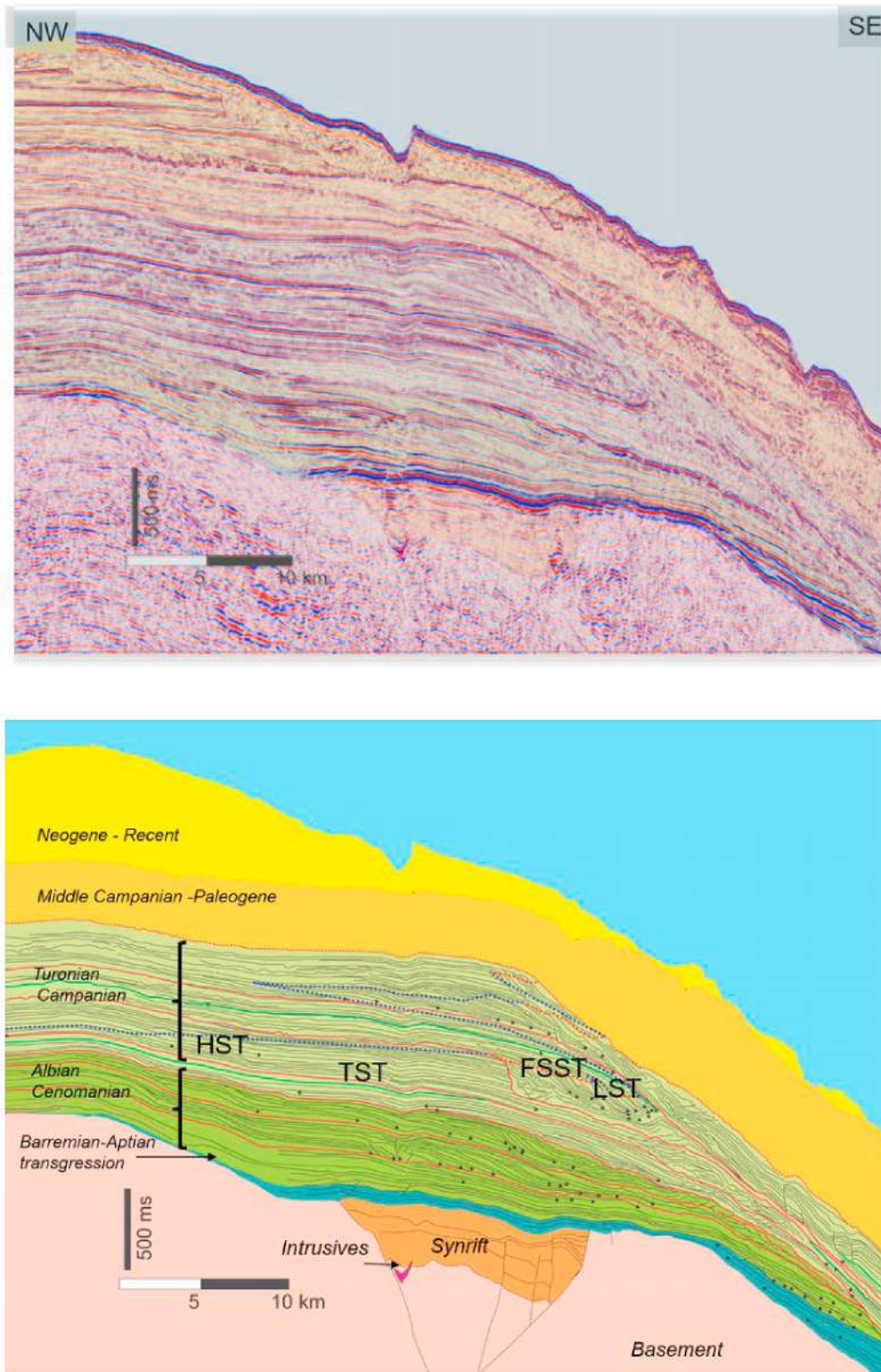


Fig. 19. a and b: uninterpreted and interpreted dip section of the outer Colorado Basin (tracing on seismic line). The blue interval represents the first marine ingression of Barremian Aptian age, covering synrift (orange) with some volcanic intrusives (red) and basement (pink). The dark green section corresponds to the clinoforms roughly equivalent in time to the Aptian – Cenomanian clinoforms described above. The light green section corresponds to the clinoforms developed during the Turonian-Campanian interval. They are separated by the Cenomanian Turonian unconformity. The dark yellow section marks the sedimentation that postdates the Campanian-Maastrichtian unconformity, followed by a regional transgressive event that extends into Danian (lower Paleocene) times. Within the Turonian- Campanian interval, different systems tracts have been recognized. After the reorganization associated with the unconformity interpreted as the Cenomanian-Turonian boundary, a transgression set the stage for the development of the structural shelf break. The topsets of the following highstand have been eroded during the next falling stage, at this location marked by a collapse of the shelf edge, partially healed during the lowstand and the transgressive system tract that followed. HST: Highstand Systems Tract; FSST: Falling Stage Systems Tract; LST: Lowstand Systems Tract; TST: Transgressive Systems Tract. (For interpretation of the references to color in this figure legend, the reader is referred to the Web version of this article.)

an overall broadening of the ocean concomitant with a wider slope promoted the onset of thermohaline currents and contourite deposits.

The Turonian –Campanian depositional system is marked by slope canyons, with meandering channels and lateral accretionary elements on the slope and frontal splays on the basin floor. On some seismic lines, sand waves can be recognized supporting the existence of nearby turbidite channels. Some chaotic reflectors within this section can also be associated to the transport of muddy sediment (e.g., slumps or mudflows), which created containers for the turbiditic events across the lower slope. In areas where sediment input from the shelf was reduced, the effect of the contour currents is more developed.

Fig. 20 is a strike section of the Salado Basin, showing canyons cut along the Cenomanian unconformity and how they evolved with time until the Maastrichtian. Here deep-water deposition is marked by canyon systems on the slope. On a 20 km spaced 2D seismic grid, the details of each canyon are beyond seismic resolution, but the fairways associated to the canyon systems as well as their continuity over time can already be seen.

7.4. Summary and discussion – change from shallow to deep water environment

The unconformity at the top of the Albian regressive unit marks a significant reorganization of the sediment dispersal systems along the SW Atlantic margin. As mentioned above, and although the exact age of this unconformity is not well constrained, regional correlation with the conjugate margin makes it likely that this event is synchronous to the 15At1 event dated as 93 M.a. (Late Cenomanian – Early Turonian), which in Africa marks the onset of deep-water circulation (Brown et al., 1995).

The immediate effect of this regional event is uplift and erosion along the margins. This can be seen on several segments beneath the current slope, where at this stage, the Albian and the top of the Aptian transgressive unit were partially eroded. At the same time, increasing spreading resulted in cooling of the oceanic crust and flexural bulging of the margin, with the development of a structurally controlled shelf break. The first canyon systems on the slope, as well as the onset of thermohaline-driven reworking are indicative of the establishment of deep-water conditions. The depositional system established at this stage continued with local variations until Maastrichtian times. Deepening of the basin and the development of the structural shelf break seem to be a blueprint for all further depositional processes until Maastrichtian – Danian times. On strike lines, the recurrence of canyon incision following approximately the same path is evident, suggesting that from Cenomanian to Maastrichtian times the margin did not experience any severe regional tilting.

8. The Campanian – Danian depositional reorganization

Spanning the Uppermost Cretaceous and Lower Paleogene (Danian) times, an unconformity along the entire South American margin, from southern Argentina (Austral Basin), onshore Argentina, Pelotas Basin (Contreras et al., 2010; Morales et al., 2017) to SE Brazilian basins (Santos, Campos and Espírito Santo) has long been recognized. It has also been identified along the Conjugate Margin in the Orange Basin (Mc Millan, 2003). The origin of this event is not clear and there may be a combination of factors contributing to its genesis. The pace of plate tectonics does not record a significant change within this timeframe, thus it is likely that there are other causes operating at regional scales. At this time, the widening of the South Atlantic precludes any direct correlation of the stratigraphic events, rather than far field climatic effects driven by the changing oceanic current systems.

In the SW Atlantic margin, this unconformity cuts deep into the slope sediments, erodes the shelf and is associated to a stacking of mass transport deposits (MTD) in deep water. Those MTDs interrelate with turbidites. In fact, erosion caused by MTDs created the relief (i.e., the container) which later filled with turbidite deposits.

8.1. Lowstand deposits on top of the near-top Cretaceous unconformity

The previous shelf and slope developed during Turonian-Campanian times was characterized by a series of forced to normal regressions, relatively thin transgressive deposits and topsets during highstands, collapses by Late Campanian times.

The collapse results in shelf exposure, deep erosion incising the sedimentary wedge down to the Albian Cenomanian section. Along the shelf break blocks of more than 20 km in length and exceeding 10 km in width collapse creating a complex toe of slope apron topography. Canyons eroding backward develop on the slope eventually linking up to deltas along the coastline, developed on a relatively narrow shelf. Gravity flows such as mass transport deposits cut deep into the sediments leaving behind depressions extending on the basin floor off the slope.

Fig. 21 is a reconstruction of processes and deposits associated with the shelf and the Campanian–Danian unconformity at the shelf edge. Based on the current seismic database, the erosive process started with mass wasting at the shelf edge and deep incision on the shelf itself. Topsets developed during previous stages were leveled down as can be seen in the inner Colorado Basin. The erosional surface caused by MTDs extended into the basin floor realm. The erosion also cut deep into the shelf, occasionally exposing Albian and even Aptian sediments. Where deposition occurred, a complex topography developed that served as entrapment mechanism for subsequent less dense flows (i.e., sandy

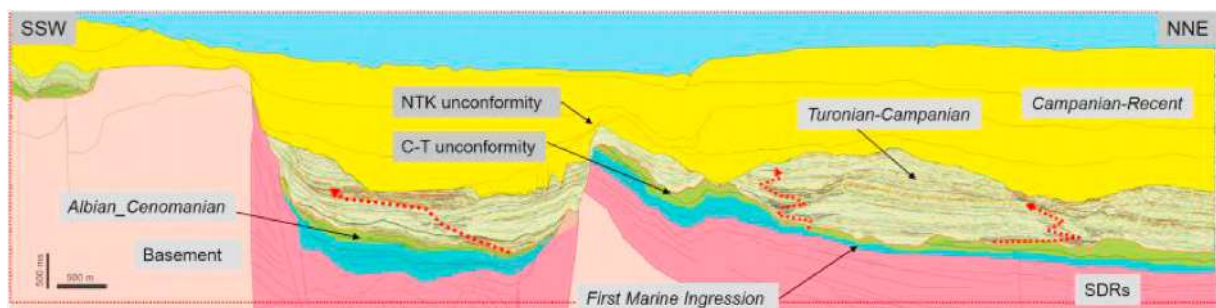


Fig. 20. Strike line of the deep water Salado Basin showing the main markers that define significant changes in the history of the SW Atlantic margin. The basement (pink) shows fractures active until Upper Cretaceous times. Laterally, SDRs overlay basement areas, following segmentation described before. On top of the SDRs, Barremian-Aptian transgressive sediments were preserved. At a paleogeographically distal position, a thin section of the shallow marine Albian-Cenomanian progradational cycles area is preserved. The Upper Cenomanian – Lower Turonian unconformity cuts deep into the older sediments, eventually eroding part of the Barremian Aptian transgressive wedge. On top the Albian-Cenomanian section, tracing shows the lateral shift and vertical stacking of slope channels laterally transitional to contourite deposits. The yellow interval represents the combined Paleogene and Neogene sections. (For interpretation of the references to color in this figure legend, the reader is referred to the Web version of this article.)

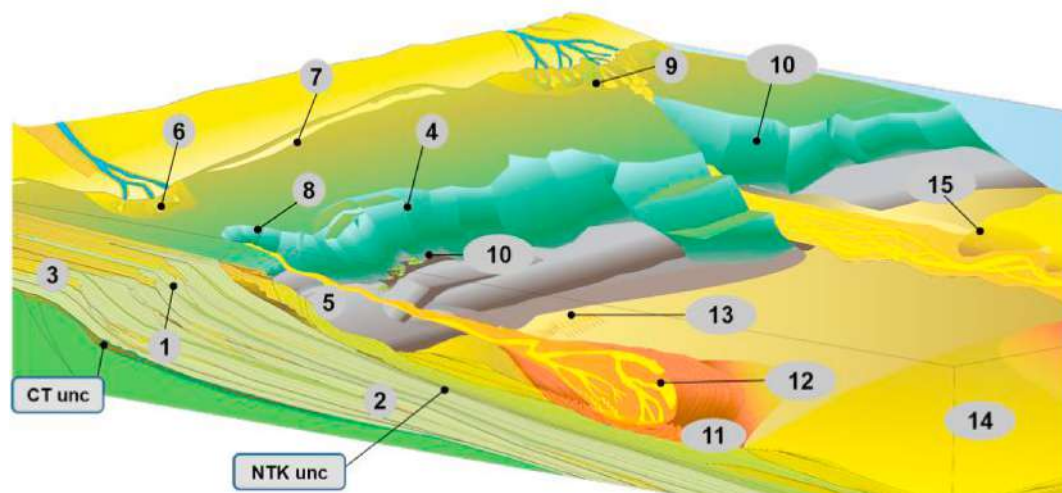


Fig. 21. Depositional elements associated with the shelf collapse during Campanian-Danian times. Pre-existing shelf: The Cenomanian – Turonian unconformity (CT unc) marks the onset of a structurally enhanced shelfbreak in a deep marine environment, with shelf edge deltas related to forced regressions (1), toe of slope and basin floor fan turbidites (2) and topsets (3) during times of highstand. Collapse features: The Campanian–Danian unconformity (NTK unc). Collapse occurs by block sliding (4) and slumping (5) along the slope. Where fluvial systems supply sediments, deltas evolve (6). Where sediment supply is low, sand is reworked by alongshore currents and constitutes coastal bars (7). During shelf collapse and basinward migrating shoreline, canyons (8) erode backward and eventually connect delta fronts with the slope. (9). Those canyons capture sediments as conduits for turbidite flows. At the base of the collapsing slope, slides and slumps leave an irregular topography which can create thicker ponded turbidite deposits. (10). Off the slope, slumps may trigger dense gravity flows which move downslope leaving erosive scars behind and, once they lose speed, create syndimentary thrusting of sediments at their front (11). The depression left behind on the seafloor is reused as a container by lower density turbidity flows depositing stacked channel turbidites (12). At the edge of these scours sand waves develop when the flow spills over them (13). Confined and unconfined turbidites are reworked by contour currents creating contourite drifts (14) and winnow out finer grained (shale) particles. Even higher energy reworking could occur when contourite currents turn into vortices at the edges of the scars left by the mass transport deposits (15).

turbidites). In the Punta del Este basin, (Uruguay), this deep-water depositional system has been analyzed and several hypotheses have been proposed to explain the erosion even off the toe of slope. A possible explanation is that strong contourite currents came into being, eroding the basin floor and creating part of the topography on which the MTDs and lower density currents were deposited (Hernández-Molina et al., 2009). This implies extremely strong thermohaline currents that would not only affect the slope but also would cause significant reworking on the basin floor. Other explanations for the erosion of the margin, from the shelf to the deep-water setting, involve tectonic instability related to supra-regional or even global events, such as the asteroid impact(s) that occurred during the same timeframe (Lerbekmo, 2014).

Fig. 22 is a paleogeographic map, where the main depositional elements developed during and immediately after the Campanian–Danian unconformity.

The key element of this interval is the eroded shelfbreak, well developed along the whole margin and cutting deep into the underlying Turonian – Campanian shelf and deep-water sequence and at some places even eroding down to the breakup unconformity on top of the SDRs, and the regional transgression that followed.

Off the eroded shelfbreak, a surface connecting the top of the incisions is interpreted as the maximum regressive surface, marking the base of the transgression that follows.

The latter event can be identified by the offlap on the slope, but less clear as a paraconcordant surface in deep waters, where only regional changes in the seismic character can help in its definition. In areas subject to higher subsidence rates, such as the Colorado and Salado Basins, shelf deposits are preserved by a thin veneer, partially eroded by the Upper Paleocene lowstand.

8.2. Maastrichtian–Danian transgression

The collapsed slope is covered by fine grained sediments, recording renewed flooding. The onset is marked by onlap on the slope, followed by a fine grained veneer recording fast flooding of the shelf and

expanding it landward, leaving the former shelf with very low supply. As a result, instability by increased water pressure produces faulting of the fine-grained wedge covering the eroded slope underneath. Transgression occurred along embayments followed the subsidence pattern of the former rift basins but they extended far inland reaching the Neuquén Basin and even connecting across the continent with the Pacific Ocean (Aguirre-Urreta et al., 2011). Between those embayments, highlands remained under the current shelf, which might locally have developed coastal rims (Fig. 22).

The overall landward shift of the coastline resulted in a starved shelf in an outer neritic environment, with little sediment supply. Clastic progradation resumed only by late Paleocene times, largely controlled by the uplift of the Andean hinterland.

By these times, the passive margin of southern South America was well evolved and a huge distance of oceanic crust separated it from the South Atlantic spreading ridge. However, volcanic events of Campanian age have been identified in the Colorado Basin, possibly extending further south. They have been drilled by two wells, Ranquel x-1 and Puelches x-1 (Fig. 1), on the shelf, where their seismic pattern was originally mistaken as reefal constructions (Lesta et al., 1978). The age of those basalts was dated with different methods: 70 ± 3 (Ar/Ar whole rock; Lesta et al., 1978) and as 74.3 ± 0.3 m.y (Ar/Ar; Lovechio et al., 2017). The basalts, which erupted in a subaqueous environment have been geochemically classified as within plate basalts, not related to the subduction along the western edge of South America, neither any ocean crust influence (Lovechio et al., 2017). On seismic lines, a clear onlap relationship between the transgressive interval on top of the unconformity and the volcanic constructions could be identified, meaning that this subaerial event occurred during the transgression. Massive clastic supply from the continent could outpace transgression only during the upper Paleocene, where a new prograding shelf break came into being.

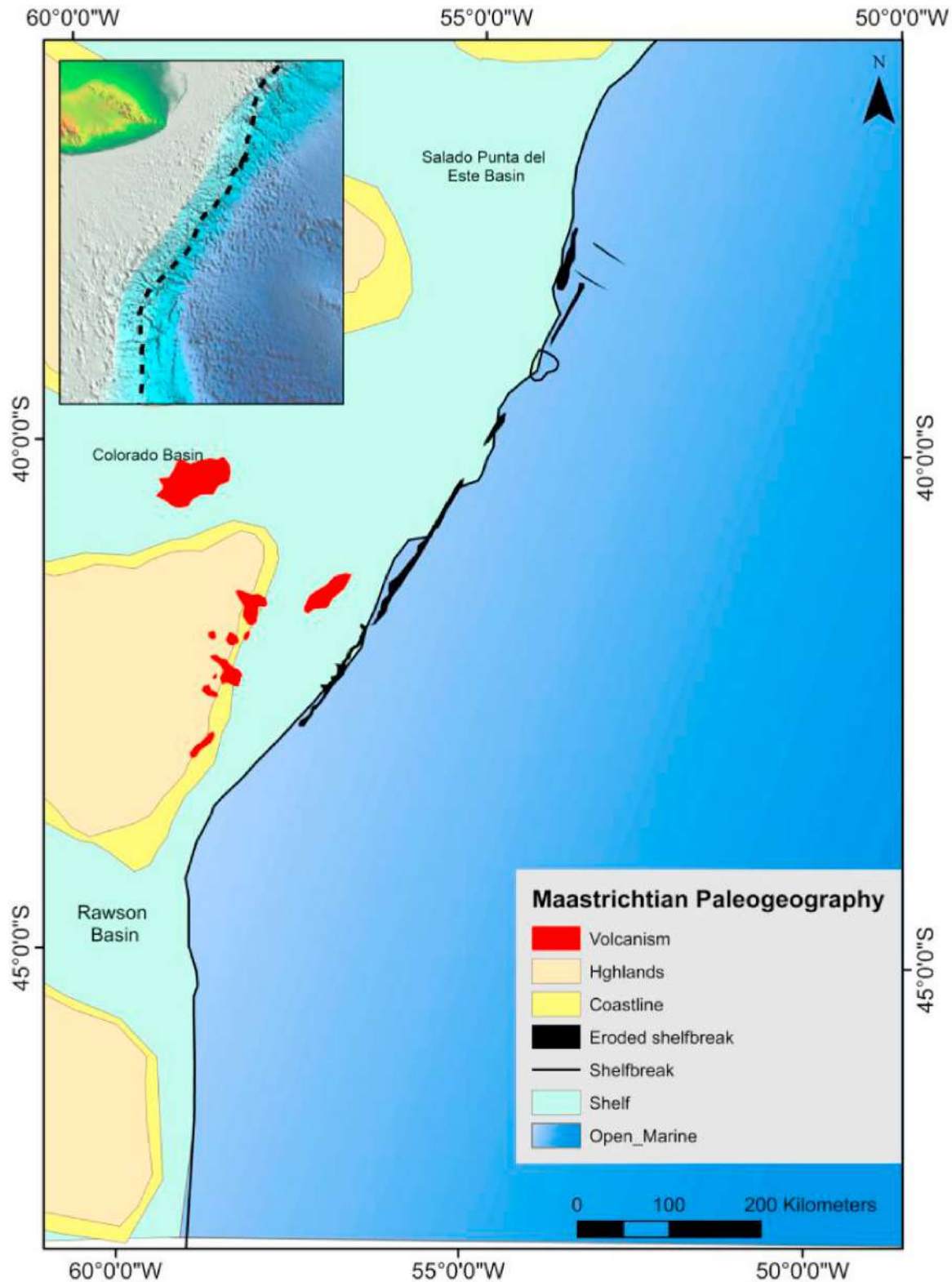


Fig. 22. Paleogeographic map showing the transgression that occurred after the Campanian – Maastrichtian unconformity. Location of the former, collapsed and eroded shelfbreak is indicated with a black line. The transgression resulted in a significant retreat of the coastline, flooding Andean foreland and intracratonic (Neuquen and Golfo San Jorge Basins respectively) and eventually connecting the South Atlantic with the Pacific across South America. However, according to the seismic data available, several areas remained exposed under the current shelf and landwards, as highlands until Neogene times.

8.3. Summary and discussion – shelfbreak collapse and regional transgression

The collapse of the shelfbreak marks the end of the Turonian–Campanian depositional system. This event has been identified even beyond the limits of the studied area. The origin of it are not clear and still under discussion. What is evident, however is the impact on the sediment dispersal systems. Slope collapse results in widespread development of huge gravity flows as mass transport deposits moving more than hundred kilometers across the basin plain. The scars they leave are later reused by lower density flows, such as high and low density turbidite flows. Where the shelf experiences lower subsidence rates (away from the basinal axes of the Colorado and Salado Basins, exposure of the shelf results in fluvial incision.

Once the sea level increases again, a thick fine-grained wedge is deposited along the slope and the adjacent shelf. Landward retreat of the coastline results in starvation and overall low sedimentation rates, while most sediment is accommodated on a broadening shelf. Resumed sedimentation during late Paleocene–Early Eocene is likely to be related to upstream controls in the Andean hinterland. In addition, in the Colorado Basin, the presence of within plate tectonic igneous activity added locally additional clastic sourcing from the eroded volcanoes.

9. Conclusions

The Cretaceous evolution of the Western South Atlantic is marked by a complex history of events which only recently could be broadly understood.

The initial nature of its volcanic margin seems to have strongly controlled the extent and paleodepth of the first marine transgression during Barremian – Aptian times.

The traditional vision of a passive margin evolving from an opening stage marked by volcanic activity during breakup has to take into account an initial shallow-marine transgression that promoted a stratigraphic shelf break during times where South America and Africa were still mechanically linked, bearing similarities in the sedimentary processes of both margins. This initial stage corresponds broadly to the Barremian/Aptian – Cenomanian interval. The depositional elements that characterize this time interval correspond to facies associated to a stratigraphic shelfbreak, with fluvial topsets, shallow water clinoforms with shelf edge deltas and toe of slope turbidite fans.

The interval marked by shallow marine depositional systems was followed by a deepening which could be a response to a broadening oceanic crust and clearing off between the Malvinas plateau and the southeastern edge of Africa by the Cenomanian–Turonian boundary, which resulted in the formation of a structural shelf break. This stage marks also the onset of a greater differentiation between the conjugated margins, and dominated the evolution of the South American margin until Campanian–Danian times. The interval is characterized by facies associated to a shelfbreak controlled by structural flexure with broader fluvial topsets, deep water clinoforms with slope canyons and levees, with winnowing associated with contourites, and basin floor fans.

The demise of this stage occurred by the end of the Cretaceous, when a widespread unconformity developed, with exposure of the shelf, erosion and deep incision along the shelfbreak, as well as slumps and gravity flows that cut deep into the lower slope and adjacent basinal plain. These depressions were reused by turbidite currents that followed, and were reworked subsequently by contour currents. The maximum regressive surface on top of this lowstand interval marks the onset of a strongly diachronous flooding of southern South America with a decrease in sedimentary input and a dominance of hemipelagic shales along the shelf and deep-water settings. This transgressive interval has been long recognized as a regional seal, which creates a significant barrier for migration from potential Cretaceous source rocks to Paleogene and Neogene reservoirs.

The impact on hydrocarbon prospectivity cannot be neglected, as

different basinal settings favor the development of distinct systems tracts and plays. While the early stages of the breakup were dominated by transgressive sands and shales, followed by the formation of an incipient relatively narrow stratigraphic shelf with high-frequency normal and forced regressions, the subsequent development of the structural shelf break marked the onset of deep-water processes with typical slope canyons and basin floor fans.

Declaration of competing interest

The authors declare that they have no known competing financial interests or personal relationships that could have appeared to influence the work reported in this paper.

Acknowledgements

This paper is the outcome of a long-term collaboration between Octavian Catuneanu and the first author, as part of the Offshore Exploration Team of YPF, together with Ricardo Gerster and Nestor Bolatti.

We would like to acknowledge permission for publication to the Exploratory Management of YPF and Facundo Fuentes for a review of the paper. We thank Istvan Csato for his editorial support, as well as two anonymous journal reviewers for their constructive comments and suggestions.

References

- Aguirre-Urreta, B., Tunik, M., Naipauer, M., Pazos, P., Ottone, E., Fanning, M., Ramos, V. A., 2011. Malarгүй group (Maastrichtian–Danian) deposits in the Neuquén Andes, Argentina: implications for the onset of the first Atlantic transgression related to western Gondwana break-up. *Gondwana Res.* 19 (2), 482–494. <https://doi.org/10.1016/j.gr.2010.06.008>.
- Arbe, H.A., 2002. Análisis Estratigráfico del Cretácico de la Cuenca Austral. In: Haller, M. J. (Ed.), *Geología y Recursos de la Provincia de Santa Cruz*, XV Cong. Geol. Arg., pp. 103–128. Relatorio.
- Ayress, M.A. y, Whatley, R.C., 2014. Early Cretaceous non-marine Ostracoda from the north Falkland basin, South Atlantic. *Palaeontology* 57, 1143–1175.
- Becker, K., Franke, D., Schnabel, M., Schreckenberger, B., Heyde, I., Krawczyk, C.M., 2012. The crustal structure of the southern Argentine margin. *Geophys. J. Int.* 189, 1483–1504. <https://doi.org/10.1111/j.1365-246X.2012.05445.x>.
- Bolli, H.M., Ryan, W.B.F., et al., 1978. Initial Reports of the Deep Sea Drilling Project, vol. 40. U.S. Government Printing Office, Washington. <https://doi.org/10.2973/dsdp.proc.40.1978>.
- Broad, D.S., Jungslager, E.H.A., Mc Lachlan, I.R., Roux, J., van der Spuy, D., 2012. South Africa's offshore Mesozoic Basins. In: *Phanerozoic Passive Margins, Cratonic Basins and Global Tectonic Maps*. <https://doi.org/10.1016/B978-0-444-56357-6.00014-7>.
- Brown, L.F., Benson, J.M., Brink, G.J., Doherty, S., Jollands, A., Jungslager, E.H.A., Keenan, J.H.G., Muntingh, A., van Wyk, N.J.S., 1995. Sequence Stratigraphy in Offshore South African Divergent Basins: an Atlas on Exploration for Cretaceous Lowstand Traps by Soekor (Pty) Ltd, vol. 41. AAPG Studies in Geology, p. 184.
- Catuneanu, O., 2006. Principles of Sequence Stratigraphy. Elsevier, Amsterdam, p. 375.
- Catuneanu, O., 2019a. Model-independent sequence stratigraphy. *Earth Sci. Rev.* 188, 312–388.
- Catuneanu, O., 2019b. Scale in sequence stratigraphy. *Mar. Petrol. Geol.* 106, 128–159. <https://doi.org/10.1016/j.marpetgeo.2019.04.026>.
- Cohen, K.M., Finney, S.C., Gibbard, P.L., Fan, J.-X., 2018. The ICS international chronostratigraphic chart. Episodes 36, 199–204. www.stratigraphy.org.
- Continanza, J., Mancada, R., Covellone, G.M., Gavarrino, A.S., 2011. Cuenca de Rawson y Valdés: síntesis del conocimiento exploratorio – Vision actual. VII Congreso de Exploración y Desarrollo de Hidrocarburos, IAPG, pp. 47–63.
- Contreras, J., Zühlke, R., Bowman, S., Bechstadt, T., 2010. Seismic stratigraphy and subsidence analysis of the southern Brazilian margin (Campos, Santos and Pelotas basins). *Mar. Petrol. Geol.* 27 (9), 1952–1980. <https://doi.org/10.1016/j.marpetgeo.2010.06.007>.
- Dummann, W., Steinig, S., Hoffmann, P., Flögel, S., Osborne, A.H., Frank, M., Herrle, J. O., Bretschneider, L., Sheward, R.M., Wagner, T., 2020. The impact of Early Cretaceous gateway evolution on ocean circulation and organic carbon burial in the emerging South Atlantic and Southern Ocean basins. *Earth Planet Sci. Lett.* 530, 115890. <https://doi.org/10.1016/j.epsl.2019.115890>.
- Franke, D. S. Neben, Ladage, S., Schreckenberger, B., Hinz, K., 2007. Margin segmentation and volcano-tectonic architecture along the volcanic margin off Argentina/Uruguay, South Atlantic. *Mar. Geol.* 244 (1–4), 46–67. <https://doi.org/10.1016/j.margeo.2007.06.009>.
- Rifting Franke, 2012. Lithosphere breakup and volcanism: comparison of magma-poor and volcanic rifted margins. *Mar. Petrol. Geol.* 43, 63–87. <https://doi.org/10.1016/j.marpetgeo.2012.11.003>.

- Galeazzi, J.S., 1998. Structural and stratigraphic evolution of the western Malvinas basin, Argentina. *AAPG (Am. Assoc. Pet. Geol.) Bull.* 82 (4), 596–636.
- Gerster, R., Welsink, H., Ansa, A., Raggio, F., 2011. Cuenca del Colorado. VII Congreso de Exploración y Desarrollo de Hidrocarburos, IAPG, pp. 65–80.
- Granot, R., Dymet, J., 2015. The Cretaceous opening of the south Atlantic Ocean. *Earth Planet Sci. Lett.* 414, 156–163. <https://doi.org/10.1016/j.epsl.2015.01.015>.
- Heine, C., Zoethout, J., Müller, R.D., 2013. Kinematics of the south Atlantic rift. *Solid Earth* 4, 215–253. <https://doi.org/10.5194/se-4-215-2013>.
- Helland-Hansen, W., Steel, R.J., Sømme, T.O., 2012. Shelf genesis revisited. *J. Sediment. Res.* 82, 133–148.
- Hernández-Molina, F.J., Paterlini, M., Violante, R., Marshall, P., de Isasi, M., Somoza, L., Rebesco, M., 2009. A contourite depositional system on the Argentine slope: an exceptional record of the influence of Antarctic water masses. *Geology* 137 (6), 507E510. <https://doi.org/10.1130/G25578A.1>.
- Hinz, K., 1981. A hypothesis on terrestrial catastrophes. Wedges of very thick oceanward dipping layers beneath passive continental margins—their origin and paleoenvironmental significance. *Geologisches Jahrbuch, Reihe E, Geophysik* 22, 3–28.
- Hinz, K., Neben, S., Schreckenberger, B., Roeser, H.A., Block, M., Goncalves de Souza, K., Meyer, H., 1999. The Argentine continental margin north of 48°S: sedimentary successions, volcanic activity during breakup. *Mar. Petrol. Geol.* 16 (1), 1–25. [https://doi.org/10.1016/S0264-8172\(98\)00060-9](https://doi.org/10.1016/S0264-8172(98)00060-9).
- Hodgson, N., Intawong, A., 2013. Derisking deep-water Namibia. *First Break* 31 (12), 91–96.
- Hofmann, P., Wagner, T., Herrle, J.O., McAnena, A., Flögel, S., 2014. Gateway opening of the south Atlantic Ocean: new high resolution insights from the Aptian to Albian Falkland plateau (DSDP 511). In: *IODP/ICDP Kolloquium 2014 at GeoZentrum Nordbayern*, 17–19.03.2014, 64–65.
- Holmes, N., Atkin, D., Mahdi, S., Ayress, M., 2015. Integrated biostratigraphy and chemical stratigraphy in the development of a reservoir-scale stratigraphic framework for the Sea Lion field area. North Falkland Basin. *Petrol. Geosci.* 21, 171–182. <https://doi.org/10.1144/petgeo2014-045>.
- Intawong, A., Esetime, P., Rodriguez, K., 2019. Observed link between folded Seaward Dipping Reflectors (SDRs) and large-scale morphology and architecture at the Early Cretaceous carbonate build-up and platform in the Orange Basin. *First Break* 37, 63–68.
- Jones, D.J.R., McCarthy, D.J., Dodd, T.J.H., 2019. Tectonostratigraphy and the petroleum systems in the Northern sector of the north Falkland basin, South Atlantic. *Mar. Petrol. Geol.* 103, 150–163. <https://doi.org/10.1016/j.marpetgeo.2019.02.020>.
- Jungslager, E.H.A., 1999. Petroleum Habitats of the Atlantic Margin of South Africa, vol. 153. Geological Society, London, Special Publications, pp. 153–168. <https://doi.org/10.1144/GSL.SP.1999.153.01.10>, 1 January 1999.
- Kollenz, S., 2015. Long-term Landscape Evolution, Cooling and Exhumation History of the South American Passive Continental Margin in NE Argentina & SW Uruguay. *Naturwissenschaftlich-Mathematischen Gesamtfakultät der Ruprecht-Karls-Universität, Heidelberg. Ph.D., Thesis.*
- Koopmann, H., Brune, S., Franke, D., Breuer, S., 2014. Linking rift propagation barriers to excess magmatism at volcanic rifted margins. *Geology* 42 (12), 1071–1074. <https://doi.org/10.1130/G36085.1>, 2014.
- Koopmann, H., Franke, D., Schreckenberger, B., Schulz, H., Hartwig, A., Stollhofen, H., Di Primio, R., 2014a. Segmentation and volcano-tectonic characteristics along the SW African continental margin, South Atlantic, as derived from multichannel seismic and potential field data. *Mar. Petrol. Geol.* 50, 22–39. <https://doi.org/10.1016/j.marpetgeo.2013.10.016>.
- Koopmann, H., Schreckenberger, B., Franke, D., Becker, K., Schnabel, M., 2014b. The late rifting phase and continental break-up of the Southern South Atlantic: the mode and timing of volcanic rifting and formation of earliest oceanic crust. In: Wright, T.J., Ayele, A., Ferguson, D.J., Kidane, T., Vye-Brown, C. (Eds.), *Magmatic Rifting and Active Volcanism*, vol. 420. Geological Society, London, Special Publications. <https://doi.org/10.1144/SP420.2>.
- Kress, P.R., Gerster, R., Bolatti, N.D., Flores, G., Arismendi, S., Lovecchio, J.P., 2019. Tectonostratigraphic Evolution of the SW Atlantic during the Cretaceous. *AAPG ICE Buenos Aires. Abstract.*
- Leckie, R.M., Bralower, T.J., Cashman, R., 2002. Oceanic anoxic events and plankton evolution: biotic response to tectonic forcing during the mid-Cretaceous. *Paleoceanography* 17 (3), 13–13–29. <https://doi.org/10.1029/2001pa000623>.
- Lerbekmo, J.F., 2014. The Chicxulub-Shiva extraterrestrial one-two killer punches to Earth 65 million years ago. *Mar. Petrol. Geol.* 49, 203–207.
- Lesta, P., Turic, M., Mainardi, E., 1978. Actualización de la información estratigráfica en la cuenca del Colorado. VII Congreso Geológico Argentino, Buenos Aires, pp. 701–713. *Actas*, 1.
- Loefering, M.J., Ankaa, Z., Autina, J., di Primio, R., Marchal, D., Rodriguez, J.F., Franke, D., Vallejo, E., 2013. Tectonic evolution of the Colorado Basin, offshore Argentina, inferred from seismo-stratigraphy and depositional rates analysis. *Tectonophysics* 604, 245–263. <https://doi.org/10.1016/j.tecto.2013.02.008>.
- Lohr, T., Underhill, J., 2015. Role of rift transection and punctuated subsidence in the development of the North Falkland Basin. *Petrol. Geosci.* 21, 85–110. <https://doi.org/10.1144/petgeo2014-2050>.
- Lovecchio, J.P., Kress, P., Rodriguez, E., Flores, G., Gerster, R., Bolatti, N., Rohais, S., Ramos, V., 2017. Caracterización del campo volcánico Campaniano-Paleoceno de la Cuenca del Colorado, Plataforma Continental Argentina, XX. Congreso Geológico Argentino, pp. 74–90.
- Lovecchio, J.P., Rohais, S., Joseph, P., Bolatti, N.D., Kress, P.R., Gerster, R., Ramos, V.A., 2018. Multistage rifting evolution of the Colorado basin (offshore Argentina): evidence for extensional settings prior to the South Atlantic opening. *Terra Nova*, *Terra Nova* 30 (5), 954–4879. <https://doi.org/10.1111/ter.12351>.
- Lovecchio, J.P., Rohais, S., Joseph, P., Bolatti, N.D., Ramos, V.A., 2020. Mesozoic rifting evolution of SW Gondwana: a polyphased subduction-related history responsible for basin formation along the Argentinean Atlantic margin. *Earth Sci. Rev.* 203, 103138. <https://doi.org/10.1016/j.earthscirev.2020.103138>.
- Max, M.D., Ghidella, M., Kovacs, L., Paterlini, M., Valladares, J.A., 1999. Geology of the Argentine continental shelf and margin from aeromagnetic survey. *Mar. Petrol. Geol.* 16 (Issue 1), 41–64. [https://doi.org/10.1016/S0264-8172\(98\)00063-4](https://doi.org/10.1016/S0264-8172(98)00063-4).
- McDermott, C., Loneragan, L., Collier, J.S., McDermott, K.G., Bellingham, P., 2018. Characterization of seaward-dipping reflectors along the south American Atlantic margin and implications for continental breakup. *Tectonics* 37 (9), 3303–3327. <https://doi.org/10.1029/2017TC004923>.
- McInerney, F.A., Wing, S.L., 2011. The paleocene-eocene thermal maximum: a perturbation of carbon cycle, climate, and biosphere with implications for the future, 39 (1), 489–516. <https://doi.org/10.1146/annurev-earth-040610-133431>.
- Mc Millan, I.K., Brink, G.J., Broad, G.S., Maier, J.J., 1997. Late Mesozoic sedimentary basins off the south coast of South Africa. In: Selley, R.C. (Ed.), *African Basins, Sedimentary Basins of the World*, vol. 3. Elsevier, pp. 319–376.
- Mc Millan, I.K., 2003. Foraminiferally defined biostratigraphic episodes and sedimentation patterns of the Cretaceous drift succession (Early Barremian to Late Maastrichtian) in seven basins on the South African and southern Namibian continental margin. *South Afr. J. Sci.* 99, 537–576.
- Menzies, M.A., Klemperer, S.L., Ebinger, C.J., Baker, J., 2002. Characteristics of volcanic rifted margins. In: Menzies, M.A., Klemperer, S.L., Ebinger, C.J., Baker, J. (Eds.), *Volcanic Rifted Margins: Boulder, Colorado*, vol. 362. Geological Society of America Special Paper, pp. 1–14.
- Morales, E., Chang, H.K., Soto, M., Correa, Santos, Veroslavsky, G., Santa Ana, H., Conti, B., Daners, G., 2017. Tectonic and stratigraphic evolution of the Punta del Este and Pelotas Basins (offshore Uruguay). *Petrol. Geosci.* 23 (4), 415–426. <https://doi.org/10.1144/petgeo2016-059>.
- Moulin, M., Aslanian, D., Unterhner, P., 2010. A new starting point for the south and equatorial Atlantic Ocean. *Earth Sci. Rev.* 98, 1–37. <https://doi.org/10.1016/j.earscirev.2009.08.001>.
- Müller, R.D., Nürnberg, D., 1991. The tectonic evolution of the south Atlantic from late Jurassic to present. *Tectonophysics* 191 (1–2), 27–53. [https://doi.org/10.1016/0040-1951\(91\)90231-G](https://doi.org/10.1016/0040-1951(91)90231-G).
- Musacchio, E., Pujana, I., Beros, C., 1990. Microfósiles continentales del J/K en Chubut y su contribución a la bioestratigrafía de la Cuenca del G.S.J., Argentina. In: *Bioestratigrafía de los Sistemas Regionales del Jurásico y el Cretácico de América del Sur*, 2. W. Volkheimer, Buenos Aires, pp. 355–371.
- Otis, R.M., Schneidermann, N., 2000. A failed hydrocarbon system – Rawson Basin. In: Mello, M.R., Katz, B.J. (Eds.), *Petroleum Systems of South Atlantic Margins*, vol. 73. AAPG Memoir, pp. 417–427.
- Planke, S., Symonds, P.A., Alvstad, E., Skogseid, J., 2000. Seismic volcanostратigraphy of large-volume basaltic extrusive complexes on rifted margins. *J. Geophys. Res.* 105, 19335–19352. <https://doi.org/10.1029/1999JB900005>.
- Quirk, D.G., Shakerley, A., Howe, M.J., 2014. A mechanism for construction of volcanic rifted margins during continental breakup. *Geology* 42, 1079–1082. <https://doi.org/10.1130/G35974>.
- Rabinowitz, P.D., LaBrecque, J., 1979. The Mesozoic South Atlantic ocean and evolution of its continental margins. *J. Geophys. Res., Solid Earth* 84 (B11), 2156–2202. <https://doi.org/10.1029/JB084iB11p05973>.
- Raggio, M.F., Gerster, R., Welsink, H., 2011. Cuenas del Salado y Punta del Este. VII Congreso de Exploración y Desarrollo de Hidrocarburos, pp. 81–96. IAPG.
- Ramos, V.A., 2008. Patagonia: a paleozoic continent adrift? *J. S. Am. Earth Sci.* 26 (3), 235–251. <https://doi.org/10.1016/j.jsames.2008.06.002>.
- Reeves, C.V., Teasdale, J.P., Mahanjane, E.S., 2016. Insight into the eastern margin of Africa from a new tectonic model of the Indian ocean. In: Nemcek, M., Rybar, S., Sinha, S.T., Hermeston, S.A., Ledvenyiova, L. (Eds.), *Transform Margins: Development, Controls and Petroleum Systems*, vol. 431. Geological Society, London, Special Publications. <https://doi.org/10.1144/SP431.12>.
- Rodrigues, S., Hernandez Molina, F.J., Kiri, A., 2021. A Late Cretaceous mixed (turbidite-contourite) system along the Argentine Margin: paleoceanographic and conceptual implications. *Mar. Petrol. Geol.* 123 <https://doi.org/10.1016/j.marpetgeo.2020.104768>.
- Seton, M., et al., 2014. Community infrastructure and repository for marine magnetic identifications. *Geochem. Geophys. Geosyst.* 15, 1629–1641. <https://doi.org/10.1002/2013GC005176> online accessed 2020 via. <http://www.soest.hawaii.edu/PT/GSFML/ML/index.html>.
- Steinig, S., Dumann, W., Park, W., Latif, M., Kusch, S., Hofmann, P., Flügel, S., 2020. Evidence for a regional warm bias in the Early Cretaceous TEX86 record. *Earth Planet Sci. Lett.* 539, 116184. <https://doi.org/10.1016/j.epsl.2020.116184>.
- Szatmari, P., Milani, E.J., 2016. Tectonic control of the oil-rich large igneous-carbonate-salt province of the South Atlantic rift. *Mar. Petrol. Geol.* 77, 567–596. <https://doi.org/10.1016/j.marpetgeo.2016.06.004>.
- Tugend, J., Gillard, M., Manatschal, G., Nirrengarten, M., Harkin, C., Epin, M.-E., Sauter, D., Autin, J., Kusznir, N., McDermott, K., 2018. Reappraisal of the magma-rich versus magma-poor rifted margin archetypes. *Geol. Soc. Spec. Publ.* 476 <https://doi.org/10.1144/SP476.9>.
- Wickens, H. de V., Mac Lachlan, I.R., 1990. The stratigraphy and sedimentology of the reservoir interval of the Kudu 9A-2 and 9A-3 B boreholes. *Communs geol Surv. Namibia* 6, 9–23.